Office de la Propriété Intellectuelle du Canada
Un organisme d'Industrie Canada

Canadian Intellectual Property Office
An agency of Industry Canada

CA 2344908 A1 2002/01/20

(21) 2 344 908

(12) DEMANDE DE BREVET CANADIEN
CANADIAN PATENT APPLICATION

(13) A1

(22) Date de dépôt/Filing Date: 2001/04/23
(41) Mise à la disp. pub./Open to Public Insp.: 2002/01/20
(30) Priorité/Priority: 2000/07/20 (09/619,877) US

(51) Cl.Int.^{7}/Int.Cl.^{7} F24F 11/02, F25D 29/00

(71) Demandeur/Applicant:
SIEMENS BUILDING TECHNOLOGIES, INC., US

(72) Inventeur/Inventor:
MCINTOSH, IAN B. D., US

(74) Agent: OYEN WIGGS GREEN & MUTALA

(54) Titre : METHODOLOGIE DE DETECTION D'ANOMALIE ET DE DIAGNOSTIC PAR MODELES POUR LES SOUS-SYSTEMES CVAC
(54) Title: MODEL BASED FAULT DETECTION AND DIAGNOSIS METHODOLOGY FOR HVAC SUBSYSTEMS

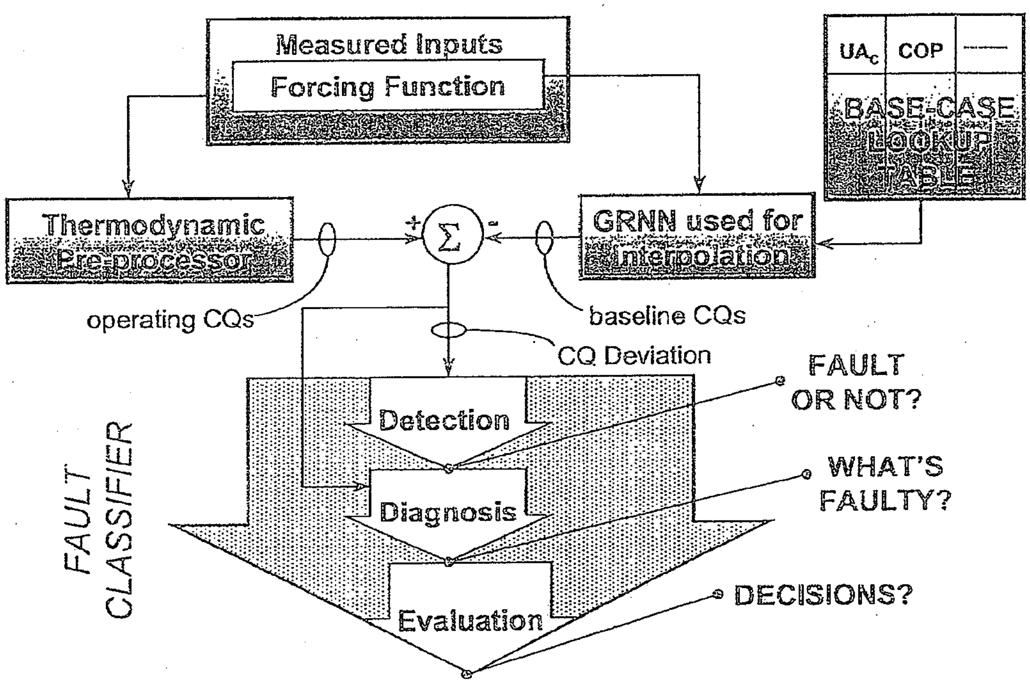

(57) Abrégé/Abstract:
A fault detection system for an HVAC system including sensors for measuring the performance of a condenser, a compressor, an evaporator, and a chiller. The fault detection system is provided with a thermodynamic preprocessor for calculating characteristic quantities (CQ's) from a plurality of measured inputs. Also provided is a base-case lookup table for storing plural first sets of CQ values generated by the thermodynamic preprocessor in an initial period in which fault-free operation of the HVAC system is assumed, a first set of CQ values being generated for each of plural different measured input values. An interpolator is provided for interpolating a set of base-case CQ values from the first sets of CQ values stored in the base-case lookup table for a given set of measured inputs. A fault-detector detects a fault when a difference between actual CQ values and base-case CQ values exceeds a predetermined threshold value for at least one of the CQ values. A fault classifier classifies a detected fault based on which ones of the actual CQ values exceed the interpolated CQ values.

MODEL BASED FAULT DETECTION AND DIAGNOSIS METHODOLOGY FOR HVAC SUBSYSTEMS

Abstract

A fault detection system for an HVAC system including sensors for measuring the performance of a condenser, a compressor, an evaporator, and a chiller. The fault detection system is provided with a thermodynamic preprocessor for calculating characteristic quantities (CQ's) from a plurality of measured inputs. Also provided is a base-case lookup table for storing plural first sets of CQ values generated by the thermodynamic preprocessor in an initial period in which fault-free operation of the HVAC system is assumed, a first set of CQ values being generated for each of plural different measured input values. An interpolator is provided for interpolating a set of base-case CQ values from the first sets of CQ values stored in the base-case lookup table for a given set of measured inputs. A fault-detector detects a fault when a difference between actual CQ values and base-case CQ values exceeds a predetermined threshold value for at least one of the CQ values. A fault classifier classifies a detected fault based on which ones of the actual CQ values exceed the interpolated CQ values.

MODEL BASED FAULT DETECTION AND DIAGNOSIS METHODOLOGY FOR HVAC SUBSYSTEMS

FIELD OF THE INVENTION

The present invention relates to a method for detecting and diagnosing faults in HVAC subsystems. More specifically, the method of the present invention detects and diagnoses faults using a combination of a physical (thermodynamic) model and a neural network.

BACKGROUND OF THE INVENTION

Vapor-compression systems account for a very significant portion of energy consumption in the industrial and commercial sectors. In large office buildings for example, it is estimated that 10% to 25% of the total electric consumption can be attributed to cooling systems alone. Furthermore, these percentages can be much greater if a chiller subsystem

is operating at low performance levels due to the presence of faults. The extensive research in Fault Detection and Diagnosis (FDD) in HVAC systems has been motivated by concerns that range from: the need to reduce power consumption and consequently energy costs; to improve comfort levels in buildings; to reduce wear on various HVAC equipment; to reduce the magnitude of greenhouse emissions; and the need to support building operators in decision-making for building optimization.

Conventional Energy Management and Control Systems (EMCS) are limited in that they do not provide the operator with the tools to diagnose faults in real-time. If effective FDD tools are designed and implemented in EMC systems, then the detection and diagnosis of various types of faults can be done automatically.

A fault, in the context of HVAC applications, is defined as an unsatisfactory or unacceptable condition in the operation of a system or subsystem. A condition is unacceptable if it is a failure or if it causes one directly or indirectly through a series of other faults. There are various types of faults, some of which are more difficult to detect and diagnose than others. The three basic fault categories, ranked in order of severity, are degradations, malfunctions and hard failures.

Degradation faults occur at a gradual rate but progressively worsen over a period of time. Overall system performance is not drastically changed until the degradation has matured beyond a critical level. Examples of system performance degradation faults are the fouling of condenser or evaporator tubes, or the clogging of filters. Notably, dirt and grime builds up on the heat transfer surfaces of the heat exchangers over time, which in turn

modifies the heat transfer coefficient of these devices. These faults gradually result in pressure drops, reduced flow rates, or higher temperature differences between the two fluids.

Malfunction faults have more immediately noticeable end effects than degradation faults, and tend to justify more immediate service. An example of this category of faults is valve leakage, sensor errors, controller breakdowns and damper stoppages are other examples. These faults usually result in failure to maintain the desired set points in temperature, pressure or flow rates.

Seized compressors and broken fan belts are examples of "hard" or "complete" failure faults. In such circumstances the impact of the fault is severe, and justifies the most immediate service. Building operators must often shut down entire subsystems in order to carry out the necessary repair.

Fault Detection and Diagnosis (FDD) is the initial step towards taking corrective or preventative measures in an HVAC system. Detection and diagnosis sometimes overlap and other times are treated separately. Fault detection involves the determination that a fault truly exists based on an observable quantity exceeding some predetermined threshold or criterion. The choice of this criterion or threshold is a tradeoff between the sensitivity of the FDD scheme and the likelihood of sounding a false alarm. Fault diagnosis is the subsequent step, that isolates the cause of the fault. Sometimes this diagnostic step does not immediately locate the root cause of the fault initially detected but may involve a series of steps that eventually converges on the cause at some later point in the diagnosis.

Once the fault has been diagnosed, fault evaluation is performed to assess whether the impact of the fault sufficient to require immediate service. In general, service should be performed whenever: (1) Comfort cannot be maintained; (2) Equipment or personal safety is compromised; (3) Environmental damage is done (e.g. refrigerant leakage); and (4) Service expense is justified by reduced energy costs.

There are several approaches to fault detection. Most, if not all, involve observation of the differences between an "actual" quantity of the system (or component) during its operation and some "predicted" value of this same quantity. The quantity under scrutiny is sometimes the "raw" measured variables (e.g., temperatures, pressures or humidity ratios that have not been pre-processed) or it may be the result of some preprocessing that transforms the measured variables collectively (in specific subsets) or individually. Some examples of the quantities used for comparison in fault detection are: Measured equipment performance *vs.* Model-based prediction of equipment performance; Measured equipment performance *vs.* Common sense expectations of acceptable performance; Measured thermodynamic states (e.g., temperatures, pressures, humidity ratios, etc.) *vs.* Model-based predicted thermodynamic states; Calculated (estimated) physical parameters for "current" performance *vs.* Calculated (estimated) physical parameters for "baseline" performance.

Similarly, there are different approaches to fault diagnosis. The result of the diagnosis is not binary as in fault detection (i.e., fault or no-fault) but involves a selection from a range of different possibilities. One such fault diagnosis approach is a rule-based diagnosis, which involves a set of rules such as directional change in temperature deviations

that may be unique to a given fault. Another approach involves comparison of physical parameters for "current" operation and "normal" operation. For example, the conductance-area product, *UA* of a condenser can be calculated from entering and leaving temperatures, and may be used to diagnose condenser fouling. Yet another approach uses a pattern recognition technique applied to "current" residuals and a matrix of "expected" residual changes associated with each fault.

Different kinds of models have been used in FDD methods. However, conventional models are unsatisfactory as they have limited general applicability. Notably, conventional models require extensive, time consuming tuning in order to tailor the model to a specific implementation. As a result, such models are not readily portable to different HVAC implementations.

Accordingly, one object of the present invention is to provide an improved model-based FDD methodology that uses a combination of a physical model and a black-box model which has general applicability to HVAC systems.

A further object of the present invention in this research is to develop an improved model-based FDD methodology for determining when and where problems occur in a centrifugal chiller system, and that is suitable for online implementation using day-to-day operating field data.

Another object is to provide an improved model which compares characteristic quantities for everyday operating conditions to a predetermined baseline of a chiller's normal

(fault-free) operation, and uses statistical hypotheses to determine if a significant deviation from this normal operation has occurred.

Yet another object is to provide a FDD method which accounts for sensor errors to provide a more robust FDD methodology.

SUMMARY OF THE INVENTION

The above-listed objects are met or exceeded by the present fault detection and diagnosis system which includes sensors for measuring the performance of a condenser, a compressor, an evaporator, which are all components of the chiller subsystem. The fault detection system further includes a thermodynamic preprocessor, a base-case lookup table, an interpolator, a fault-detector and a fault classifier.

The thermodynamic preprocessor, which is preferably a software routine executed on a computer or the like, calculates characteristic quantities (CQ's) from a plurality of measured inputs. The base-case lookup table stores plural first sets of CQ values generated by the thermodynamic preprocessor in an initial period in which fault-free operation of the HVAC system is assumed, a first set of CQ values being generated for each of plural different measured input values.

The interpolator generates a set of interpolates base-case CQ values for a given set of measured inputs from among the first sets of CQ values stored in the base-case lookup table that is stored in memory of the computer. The fault-detector, which is preferably a software routine executed on a computer or the like, detects a fault when a difference

between actual CQ values, calculated by the thermodynamic preprocessor for a given set of measured inputs, and the interpolated set of base-case CQ values for the given set of measured inputs exceeds a predetermined threshold value for at least one of the CQ values. The fault classifier, which is preferably a software routine executed on a computer or the like, classifies a detected fault based on which ones of the actual CQ values exceed the interpolated CQ values.

BRIEF DESCRIPTION OF THE DRAWINGS

FIGURE. 1 is block diagram showing the overall structure of the model-based fault detection and diagnosis system of the present invention;

FIG. 2 is a block diagram showing the inputs and some of the outputs of the thermodynamic preprocessor of the present invention;

FIG. 3 is an EES (Engineering Equation Solver) procedure used to determine the logarithmic mean temperature difference between the evaporator saturation temperature (T_evap), the chilled water supply temperature (T_chws), and the chilled water return temperature (T_chwr);

FIG. 4 is an EES procedure used to determine the logarithmic mean temperature difference between the condenser saturation temperature (T_cond), the condenser water supply temperature (T_cws) and the condenser water return temperature (T_cwr)

FIG. 5 depicts equation sets for the condenser side input data used by the EES procedure of FIG. 4;

FIG. 6 are EES program statements for inputting data used in the equations of FIGs. 3 and 8;

FIG. 7 are EES program statements for inputting data used in the equations of FIG. 9 and FIG. 10;

FIG. 8 are equations used to determine evaporator related characteristic quantities;

FIG. 9 are equations used to determine compressor related characteristic quantities;

FIG. 10 are equations used to determine condenser related characteristic quantities;

FIG. 11 is an expansion valve equation used by the EES code in FIG.8;

FIG. 12 is a list of thermodynamic properties and conversion constants used by the EES code in FIGs. 8-10;

FIG. 13 is a schematic of a chiller showing the location of each of the sensors used to obtain the measured inputs;

FIG. 14 illustrates the structure of a single neuron unit;

FIG. 15 shows the general architecture of a interconnected neural network with several neurons, links and layers;

FIGs. 16A-C are graphs illustrating how different smoothing parameters are used in smoothing a trained GRNN;

FIG. 17 shows the neural network architecture of the GRNN algorithm of the present invention;

FIG. 18 shows the sensitivity of *UA* when used to detect flow rate reductions;

FIG. 19 shows the sensitivity of the entering/leaving water temperature difference when used to detect flow rate reductions;

FIG. 20 shows the sensitivity of UA when used to fouling of the heat exchanger tubes;

FIG. 21 shows the sensitivity of APPR when used to detect fouling of the heat exchanger tubes;

FIG. 22 shows the sensitivity of $\eta_{isentropic}$ when used to detect compressor faults;

FIG. 23 shows the sensitivity of η_{motor} when detecting motor or transmission faults.

FIG. 24 shows the sensitivity of UA_c, and $APPR_c$ when detecting fouling faults;

FIG. 25 shows the sensitivity of compressor isentropic efficiency when detecting compressor faults;

FIG. 26 shows the sensitivity of motor efficiency when detecting motor faults; and

FIG. 27 is a chart summarizing the relationships illustrated in FIGs. 18-26.

DETAILED DESCRIPTION OF THE PREFERRED EMBODIMENTS

The inventor of the present invention discovered that it is difficult to detect and diagnose a fault in a chiller subsystem from raw data collected from sensors. Notably, it is difficult to set a meaningful fault threshold which is applicable to different chill subsystem implementations, i.e., is not customized for a particular implementation. To overcome this problem, the inventor of the present invention utilize a series of characteristic quantities which are calculated from the raw data using well known thermodynamic principles. The use of such characteristic quantities eliminates the need to individually tune the system of the present invention for any given HVAC installation.

Importantly, the inventor of the present invention discovered that some characteristic quantities (CQs) are more sensitive than others in detecting certain faults. Table I below, summarizes the outputs (characteristic quantities) and the inputs used to determine them.

The sensitivity of each CQ value to a given fault was determined by simulating various faults in a controlled experiment. Each fault condition in addition to a base case (no-fault) condition was simulated. Table II below pairs particular fault conditions with potential CQs that may be used for their detection. The inventor of the present invention developed a system for detecting and diagnosing faults utilizing the relationship summarized in Table II.

TABLE I

	(Raw Data)		Outputs (Characteristic Quantities)	
1	T_{chws}	chilled water supply temp. (°F)	$APPR_e$	evaporator heat exchanger approach (°F)
2	T_{chwr}	chilled water return temp. (°F)	$APPR_c$	condenser heat exchanger approach (°F)
3	T_{cws}	condenser water supply temp. (°F)	CHWTD	chilled water temp. difference (°F)
4	m_{chw}	chilled water flow rate (gpm)	CWTD	condenser water temp. difference (°F)
5	m_{cw}	condenser water flow rate (gpm)	UA_c	condenser conductance-area product (Btu/hr-°F)
6	T_{evap}	evaporator saturation temp. (°F)	UAe	evaporator conductance-area product (Btu/hr-°F)
7	T_{cond}	condenser saturation temp. (°F)	$\eta_{isentropic}$	isentropic heat transfer coefficient (Btu/hr-ft^2-°F)
8	T_2	compressor discharge temp. (°F)	η_{motor}	motor/transmission heat transfer coefficient (Btu/hr-ft^2-°F)
9	P	compressor power	$COP_{overall}$	overall coefficient of performance
10			COP_{comp}	compressor coefficient of performance

TABLE II

Fault Type	**Sensitive CQs**
(1) Condenser water flow reduction	UA_c, $APPR_c$, $CWTD$
(2) Chilled water flow reduction	UA_e, $APPR_e$, $CHWTD$
(3) Evaporator tube fouling	UA_e and $APPR_e$
(4) Condenser tube fouling	UA_c and $APPR_c$
(5) Compressor internal faults	P, COP_{comp} and $\eta_{isentropic}$
(6) Motor/Transmission faults	P, $COP_{overall}$ and η_{motor}

FIG. 1 is a block diagram of the overall structure of the model-based fault detection and diagnosis methodology of the present invention. The fundamental components

along with their links to other components and flow of information for fault detection and diagnosis are depicted.

There are two sources of data used in this methodology, operating CQ's calculated on-the-fly, and base-case CQ's which are interpolated from data stored in a look-up table. As shown in FIG. 1, measured inputs (and forcing functions), such as the chilled water supply temperature of the chiller and cooler water are fed to both the thermodynamic preprocessor 100 and the interpolator 102. The thermodynamic preprocessor 100 uses the measured inputs to generate the characteristic quantities (CQs). The operating CQ's are compared with base-case CQ's which are interpolated from empirical data stored in a base case lookup table 104.

The look-up table 104 stores values of CQ's that were generated during a period in which fault-free operation of the chiller is assumed. The interpolator 102 interpolates normal (base-case) CQ's from the data stored in the look-up table 104. The process for obtaining the operating and base case CQ values will be explained in detail below.

The streams of operating and base-case CQ data are compared and errors (residuals) are computed. The residuals are fed to the Fault Classifier section 108 where the appropriate statistical analyses are employed to determine the significance of these errors. If they are indeed statistically significant, a fault detection alarm is produced. Otherwise, monitoring continues with the assumption that the chiller process is operating normally and that no faults are present.

If faults are detected, the diagnostic classifier determines the type of fault and its likely location within the chiller. The CQs used in the methodology of the present invention were specifically selected to make isolating the fault location easier. As noted above, the inventor of the present invention discovered that certain CQs are sensitive to some faults and not to others. Thus, the careful selection of CQs makes it possible to distinguish between fault types.

Once faults are detected and diagnosed, they are subsequently evaluated to determine the most suitable action to take. Fault Evaluation deals with comfort, safety, environment and economic issues. Action could be taken whenever: (1) comfort cannot be maintained, (2) equipment or personal safety is compromised, (3) environmental damage occurs (e.g. refrigerant leakage), or (4) reduced energy costs justify the service expense.

In order to conduct on-line FDD using day-to-day operating data, it is desirable to have a model that can generate CQ's without the need for any manual intervention. The thermodynamic preprocessor 100 requires only eight measurement variables to generate the necessary CQ's immediately. See FIG. 2. Sets of CQ's are generated at two different time periods. As will be explained below, plural first sets of CQ variables (base-case CQ's), representative of normal (fault-free) system operating conditions, are generated and stored in the look-up table 104 during a preliminary period when a sufficiently wide range of loads is covered. A second set of CQ data (operating CQ's) is generated "on-the-fly", i.e., generated contemporaneously with the receipt of the measured inputs to reflect the existing

state of the system, after the preliminary period has expired, and is compared with the first set of CQ variables to determine if faults have occurred.

Both sets of CQ variables are generated in the same manner, the only difference being the time period in which each set is generated. Namely, the plural sets of base-case CQ's are generated during a preliminary period in which fault-free operation of the chiller is carefully controlled. The operating set of CQ's are generated on-the-fly after the base-case CQ sets have been stored in the look-up table 104.

The thermodynamic preprocessor 100 generates the operating CQ's using a thermodynamic data reduction program which was written in EES, an Engineering Equation Solver Software developed by S.A. Klein and F.L. Alvarado, F-Chart Software, Inc. The EES program is particularly suited for solving thermodynamic equations; however, one of ordinary skill in the art will appreciate that other programming languages or software packages may also be used.

The thermodynamic data reduction program consists of two procedures (FIGs. 3 and 4) and equation sets for the condenser side input data (FIG. 5), evaporator side input data (FIG. 6), compressor input data (FIG. 7), evaporator equations (FIG. 8), compressor equations (FIG. 9), condenser equations (FIG. 10), expansion valve equations (FIG. 11) and for the thermodynamic properties and conversion constants (FIG. 12). It should be noted that the thermodynamic data reduction program uses general thermodynamic principles, and is not specifically tuned for a specific chiller subsystem. For this reason, the CQ's have general applicability to all chiller subsystems.

A procedure statement heads each procedure (FIGs. 3 and 4), and identifies the name and arguments of the procedure. Thus, the statement "Procedure LMTD_e(T_chws, T_chwr, T_evap: LMTDe, T_we, ln_arg_e)" defines a procedure LMTD_e and a series of arguments (inputs and outputs).

Table I, above, lists the input/outputs of the thermodynamic data reduction program. Moreover, FIG. 13 is a schematic of a chiller showing the location of each of the sensors used to obtain the measured inputs.

The procedures (FIGs. 3 and 4) utilize function calls in which the function max(x,y) returns the larger of the two arguments (x, y). Thus, max(0, -2) returns "0". Correspondingly, the function ln(x) returns the natural log of argument x.

The procedure LMTD_e (FIG. 3) is used to determine the logarithmic mean temperature difference between the evaporator saturation temperature (T_evap), the chilled water supply temperature (T_chws), and the chiller water return temperature (T_chwr). The built-in EES error procedure halts the calculations if T_evap is greater than T_chws or if T_chws is greater than T_chwr.

The procedure, LMTD_c (FIG. 4) is used to determine the logarithmic mean temperature difference between the condenser saturation temperature (T_cond), the condenser water supply temperature (T_cws) and the condenser water return temperature (T_cwr). The built-in EES error procedure halts the calculations if T_cond is less than T_cwr or if T_cwr is less than T_cws.

In developing the base case look-up table, measurement data for a wide variety of base-case operating conditions is compiled in a table which is accessed by the thermodynamic data reduction program. As will be appreciated by one of ordinary skill in the art, it is advantageous to collect measurement data for as wide a variety of operating conditions as possible in order to improve the accuracy of the interpolated CQ values. For example, it is desirable to calculate base-case CQ values for various times of day for both workdays and non-workdays, different weather conditions (ambient temperature, sunlight, winds, humidity), etc to fully reflect the wide range of heating/cooling loads encountered by the system.

In FIGs. 5-7, the statement lookup(x, y) "F" is used to access entry "x" in the lookup table and assign the returned value to variable "y". The units for each variable accessed from the lookup table is provided in the comments following each lookup statement. Thus, in the above example, the units are in degrees Fahrenheit.

As noted above, a first set of CQ variables, representative of normal (fault-free) system operating conditions, is generated during a preliminary period when a sufficiently wide range of loads is covered. It is assumed that sufficient data are collected and that there are no major unforeseen systematic changes during data collection.

Fault detection is performed by comparing each respective operating CQ variable with a corresponding base-case CQ variable. Each set of CQ variables stored in the lookup table 104 includes at least eight (of the nine) input and ten (of the output variables listed in Table I.

As will be appreciated by one of ordinary skill in the art, there are many different combinations of input variables, whereas the look-up table only contains a relatively small subset of the possible combinations. Consequently, it is unlikely that a given set of eight measured inputs acquired on-the-fly will directly match one of the sets of input variables stored in the look-up table 104. Accordingly, the interpolator 102 determines a set of base-case CQ variables through a process of interpolation.

The inventor of the present invention investigated a number of different interpolation schemes. Linear interpolation and regression against power form relations were found to be inaccurate and not general. According to a preferred embodiment, Neural Network architecture was found to be well suited to the interpolation. However, one of ordinary skill in the art will appreciate that other interpolation methods may be substituted.

Neural network models are inspired by the human thought processes. Over 100 billion biological neurons are present in the human brain. The connections between these neurons are called synapses and when the brain learns their strength is modified.

Analogously, artificial neural networks contain artificial neurons that are connected via one-way information conduits called links. Weights are associated with these links that control the magnitude of the input signal entering the artificial neuron. These link weights simulate the physical and neuro-chemical characteristics of the biological synapse. Each artificial neuron in the network functions by first summing its scaled inputs and then applying a non-linear function to this sum to generate an output. FIG. 14 illustrates the

simple structure of a single neuron unit and FIG. 15 shows the general architecture of a interconnected network with several neurons, links and layers.

A layer is a grouping of neurons and are of three basic types. The input layer receives data from outside of the network, the output layer holds the network's final computational results and any layers in between these two are called hidden layers.

A basic feature of neural networks is that they learn by example and are never programmed. Therefore, in order to train a network, it must be presented with a data sample that contains the inputs and their corresponding outputs. By an iterative process, the network gradually learns the input-output relationship and then, depending on the application, is used for prediction, correction or pattern recognition. Once trained, they can resolve numeric problems that are otherwise solved by conventional regression analysis. In the network, the inputs are equivalent to the independent variables used in regression, the dependent variables become the outputs and the observations are the sample patterns used for training the network.

Neural networks fall into the two basic categories of: *supervised* networks and *unsupervised* networks. Supervised networks are those that make predictions, classify patterns or make decisions based on a set of learned inputs and outputs. Some examples of these are the Probabilistic Neural Networks (PNN), the General Regression Neural Networks (GRNN) and Back Propagation Networks. These kinds of networks are trained to make predictions, classifications, or decisions when given a large enough number of accurate classifications or predictions from which it can learn.

Unsupervised networks, without being taught how to categorize, are able to classify a given number of input and output patterns into a specified number of categories. They do this by clustering the training patterns using their proximity in n dimensional space where n is the number of inputs. The network usually clusters the data into the maximum number of categories it is presented with. Kohonen Networks are examples of this network type.

The GRNN is one type of neural network that is well suited to interpolation. It is based on the estimation of a probability density function of a vector random variable, X, and a scalar random variable, Y. If the joint probability density function of these variables are both known then the conditional probability density function and the expected value can be computed. The estimated value of Y for a given X is presented in the following general regression equation:

$$E[Y \setminus X] = \frac{\int_{-\infty}^{\infty} Yf(X,Y)dy}{\int_{-\infty}^{\infty} f(X,Y)dy} \qquad (1)$$

where

$E[Y \setminus X]$ = conditional mean of Y on X

$f(X,Y)$ = known joint continuous probability density function

The probability density function, $f(X,Y)$, is estimated from sample observations of X and Y when it is unknown. For a non-parametric estimate of $f(X,Y)$, the Parzen estimation $f'(X,Y)$, is used by the GRNN. It is defined by the following equation for the observed sample observations, X_i and Y_i of the vector X and scalar Y:

$$f'(X,Y)=\frac{1}{(2\pi)^{\frac{p+1}{2}}\sigma^{p+1}}\cdot\frac{1}{n}\sum_{i=1}^{n} f_X f_Y \qquad (2)$$

where

$$f_X=\exp\left[-\frac{(X-X_i)^T(X-X_i)}{2\sigma^2}\right] \qquad (3)$$

and

$$f_Y=\exp\left[-\frac{(Y-Y_i)^2}{2\sigma^2}\right] \qquad (4)$$

and

n = the number of sample observations

p = the dimension of the X vector

σ = the standard deviation (or smoothing parameter)

An estimate for the desired mean of Y at any given X is derived in Equation (5) by combining Equations (1) and (2) and performing the integration after first interchanging the integration and summation operation.

$$\hat{Y}(X) = \frac{\sum_{i=1}^{n} Y_i \exp\left(-\frac{D_i^2}{2\sigma^2}\right)}{\sum_{i=1}^{n} \exp\left(-\frac{D_i^2}{2\sigma^2}\right)} \tag{5}$$

where, the scalar function D_i^2 is given by:

$$D_i^2 = (X - X_i)^T (X - X_i) \tag{6}$$

The main algorithm of the GRNN model is expressed by Equations (5) and (6). The estimate $\hat{Y}(X)$ is a weighted average of all the observed samples, Y_i, where each sample is weighted in an exponential manner according to the Euclidean distance, D_i, from each X_i. This appropriate weighting is explained by the inversely proportional relationship between the expression $\exp\left(-\frac{D_i^2}{2\sigma^2}\right)$ and D_i. That is, as D_i increases, $\exp\left(-\frac{D_i^2}{2\sigma^2}\right)$ decreases and vice-versa. An optimum value for the smoothing parameter, σ, is determined using iterative or

genetic adaptive methods. Iterative methods such as the *Holdout* method and the *Wiggle* method are well known by those of ordinary skill in the art, and do not form part of the present invention. Larger values of σ improve smoothness of the regression surface. Notably, σ must be greater than 0 and can usually range from .01 to 1 with good results.

FIGs. 16A-C illustrates how different smoothing parameters are used in smoothing a trained GRNN. In this example, one input value is used to predict one output value. As shown in the graph, of the forty input and output patterns only input patterns 10, 20, and 30 produce an output value of 1.

FIG. 17 represents the neural network architecture of the GRNN algorithm of Equations (5) and (6). The Euclidean distance, D_i, is computed by the links between the input layer and the first hidden layer. Based on observed samples, X_i, and smoothing parameter, σ, the expression,

$$\exp\left(-\frac{D_i^2}{2\sigma^2}\right)$$

is computed. A node in the second hidden layer takes the sum of the exponential values of all samples. In other nodes of this same layer, the products of the exponential values and the corresponding observed Y_i for each sample observation are computed. The node in the third hidden layer computes the sum of all these product values, which is then supplied to the output node where the ratio between it and the previous sum is calculated.

The suitability of the GRNN, however, is attributed to several important features and makes it convenient for online implementation. In the GRNN network only a single parameter is estimated. Unlike other networks, a once through, non-iterative training process with a highly parallel structure is involved. Compared to conventional regression analysis, the specification of the underlying regression function, bounds of the independent variables, initial convergence values and convergence criteria are not required beforehand. Additionally, the algorithm provides smooth transitions from one observed value to another even with sparse and noisy data in a multidimensional measurement space and can be used for any regression problem where an assumption of linearity is not justified.

Since the thermodynamic and the GRNN models involve functions and variables in a multi-dimensional space, it is important to know what the truly independent measurement variables are. Here, the term *independent* refers to those variables that are forcing functions of the chiller process. Information about variable independence is necessary for understanding the available data, achieving greater insight to data manipulation, accurately assigning inputs and outputs, and successfully training the GRNN model to be able to predict normal system behavior. For the chiller process, only five measurement variables may be considered independent. This number is determined from studying the various equations that define the chiller process more closely in the discussion that follows.

An overall energy balance of the entire refrigeration system is:

$$Power = \dot{Q}_{evap} - \dot{Q}_{cond} \tag{7}$$

$$\dot{Q}_{cond} = \dot{m}_{cw} C_{pw} (T_{cwr} - T_{cws}) \tag{8}$$

$$\dot{Q}_{cond} = \dot{m}_{ref} (h_2 - h_3) = \dot{m}_{ref} \Delta h_{ref,cond} \tag{9}$$

The enthalpy difference, $\Delta h_{ref,cond}$, between the entering and leaving refrigerant in the condenser is a function of the condenser saturation temperature, T_{cond}:

$$\Delta h_{ref,cond} = f(T_{cond}) \tag{10}$$

$$\dot{Q}_{evap} = \dot{m}_{chw} C_{pw} (T_{chwr} - T_{chws}) \tag{11}$$

$$\dot{Q}_{evap} = \dot{m}_{ref} (h_4 - h_1) = \dot{m}_{ref} \Delta h_{ref,evap} \tag{12}$$

Here, the enthalpy difference, $\Delta\eta_{ref,evap}$, between the entering and leaving refrigerant in the evaporator is a function of the evaporator saturation temperature, T_{evap}:

$$\Delta h_{ref,evap} = f(T_{evap}) \tag{13}$$

In addition to the above relations, the following relations for the chiller Power and Capacity, $\dot{Q}_{evap}$ are available from chiller manufacturers' experiments:

$$Power = f(T_{evap}, T_{cond}) \tag{14}$$

$$\dot{Q}_{evap} = f(T_{evap}, T_{cond}) \tag{15}$$

Equations (7) to (15) fully define the thermodynamic data reduction model. An inventory of the number of equations and the number of unknowns yield nine and fourteen, respectively. Thus the difference between these two numbers tells us that five variables must be independently measured for these model equations to work.

The inventor of the present invention selected the following five independent measurement points condenser supply temperature, T_{cws}, the chilled water supply temperature, T_{chws}, the chilled water return temperature, T_{chwr}, the condenser water flow rate, $\dot{m}_{cw}$, and the chilled water flow rate, $\dot{m}_{chw}$. However, the selection of other independent measurement points is contemplated and falls within the scope of the present invention.

The condenser water supply temperature, T_{cws} and the chilled water return temperature, T_{chwr} are the entering water temperatures to the chiller subsystem. The chiller subsystem has no direct effect on the magnitudes of these two water streams until after they cross the system boundary. Therefore, the temperatures, T_{chwr} and T_{cws} are independent. They represent only a part of the building load and heat rejection, respectively. The flow rates, $\dot{m}_{chw}$ and $\dot{m}_{cw}$, are additional required independent variables. The final measurement

variable, the chilled water supply temperature, T_{chws}, is termed independent because its magnitude is associated with a control set-point.

The essence of the Fault Detection scheme relies on the determination that a fault truly exists based on the deviation of a Characteristic Quantity (CQ) exceeding some predetermined threshold or criterion. This deviation is measured from an established base case representing normal operating conditions.

As described above, the CQ values are computed from measurement data gathered from sensors. Due to the many perturbations that exist, there is an inevitable chain of causes and effects that occur and form the basis for uncertainties in the measurement data. Some of the factors that may cause perturbations are power supply variance, hysteresis, precision and bias errors and general instability. These factors contribute to the accuracy ratings of the measurement sensors and therefore, are factors that contribute to the uncertainties in CQ deviations. These uncertainties in CQs determine the threshold and thus the sensitivity for fault detection. A tighter uncertainty region corresponds to more sensitive detection.

Numerous situations involve the computation of an important quantity, Y, instead of its direct measurement. If such a quantity is determined from N other directly measured quantities $X_1, X_2, \ldots, X_N$, a functional relation between these quantities and Y may be expressed as $Y = f(X_1, X_2, \ldots, X_N)$. This function f not only expresses a physical law but

a measurement process. In fact, all the quantities that could contribute a significant uncertainty to the measurement results are accounted for by f.

Furthermore, if $\hat{Y}$ represents the estimate of the output quantity, Y, and $x_1, x_2, \ldots, x_N$ are input estimates for the values of the N input measurements, $X_1, X_2, \ldots, X_N$, then $\hat{Y}$ can be expressed as $\hat{Y}=f(x_1,x_2,\ldots,x_N)$. In order to obtain the combined standard uncertainty, $u_c(\hat{Y})$ of the computation result $\hat{Y}$ (an estimated standard deviation of the result), a first-order Taylor series approximation of $Y=f(X_1,X_2,\ldots,X_N)$ is performed. This gives the following expression known as the Law of Propagation of Uncertainty:

$$u_c(\hat{Y})=\left[\sum_{i=1}^{N}\left(\frac{\partial f}{\partial x_i}\right)^2 u^2(x_i)+2\sum_{i=1}^{N-1}\sum_{j=i+1}^{N}\frac{\partial f}{\partial x_i}\frac{\partial f}{\partial x_j}u(x_i x_j)\right]^{1/2} \qquad (16)$$

where

$$\frac{\partial f}{\partial x_i}=\left.\frac{\partial f}{\partial X_i}\right|_{X_i=x_i} = \text{sensitivity coefficients}$$

$u(x_i)$ = standard uncertainty associated with the input estimate, x_i

$u(x_i,x_j)$ = estimated covariance associated with x_i and x_j

If the individual measurement inputs are assumed uncorrelated and random, then the covariance term is zero and $u_c(\hat{Y})$ is simplified to:

$$u_c(\hat{Y}) = \left[\sum_{i=1}^{N}\left(\frac{\partial f}{\partial x_i}u(x_i)\right)^2\right]^{1/2} \qquad (17)$$

By manner of example, two CQs that are sensitive to tube fouling in the condenser are its approach, $APPR_c$, and conductance-area product, UA_c. Using the simplified form of the uncertainty propagation law in Equation (17), expressions can be derived for the uncertainties in UA_c and $APPR_c$.

Equation (18) that defines the conductance-area product of the condenser, UA_c, in terms of four independently measured variables and a fluid property, C_{pw}. This property is the specific heat of water and actually varies with temperature conditions but was assumed constant for this application since the range of variation is insignificant.

$$UA_c = \dot{m}_{cw} \cdot C_{pw} \cdot \ln\left(\frac{T_{cond} - T_{cws}}{T_{cond} - T_{cwr}}\right) \qquad (18)$$

The UA_c is a $f(T_{cws}, T_{cwr}, T_{cond}, \dot{m}_{cw})$. Equation (16) was used to express the most probable uncertainty in UA_c as:

$$u_c(UA_c)=\left[\left(\frac{\partial UA_c}{\partial T_{cws}}\cdot u(T_{cws})\right)^2+\left(\frac{\partial UA_c}{\partial T_{cwr}}\cdot u(T_{cwr})\right)^2+\left(\frac{\partial UA_c}{\partial T_{cond}}\cdot u(T_{cond})\right)^2+\left(\frac{\partial UA_c}{\dot{m}_{cw}}\cdot u(\dot{m}_{cw})\right)^2\right]^{1/2} \qquad (19)$$

where,

$$\frac{\partial UA_c}{\partial T_{cws}}=\frac{-\dot{m}C_{pw}}{(T_{cond}-T_{cws})} \qquad (20)$$

$$\frac{\partial UA_c}{\partial T_{cwr}}=\frac{-\dot{m}C_{pw}}{(T_{cond}-T_{cwr})} \qquad (21)$$

$$\frac{\partial UA_c}{\partial T_{cond}}=\frac{\dot{m}C_{pw}(T_{cws}-T_{cwr})}{(T_{cond}-T_{cwr})(T_{cond}-T_{cws})} \qquad (22)$$

$$\frac{\partial UA_c}{\partial m_{cw}}=C_{pw}\cdot\ln\left(\frac{(T_{cond}-T_{cws})}{(T_{cond}-T_{cwr})}\right) \qquad (23)$$

and, $u(T_{cws}), u(T_{cwr}), u(T_{cond})$ and $u(\dot{m}_{cw})$ are the uncertainties of the measured condenser water supply temperature, condenser water return temperature, refrigerant condenser saturation temperature and the water mass flow rate, respectively. These uncertainties are equivalent to the accuracy of the measurement sensors.

The approach, $APPR_c$ is a $f(T_{cwr}, T_{cond})$. The most probable uncertainty in $APPR_c$ may be expressed as:

$$u(APPR_c) = \left[\left(\frac{\partial APPR_c}{\partial T_{cwr}} \cdot u(T_{cwr}) \right)^2 + \left(\frac{\partial APPR_c}{\partial T_{cond}} \cdot u(T_{cond}) \right)^2 \right]^{1/2} \qquad (24)$$

where

$$\frac{\partial APPR_c}{\partial T_{cwr}} = -1 \qquad (25)$$

and

$$\frac{\partial APPR_c}{\partial T_{cond}} = +1 \qquad (26)$$

For the threshold analysis, only precision errors were used. The following sensor precision errors, developed using time series analysis, were used to evaluate the effect of error on CQ:

- Temperature sensor: ±0.3°F and ±0.6°F
- Water flow rate sensor: ±5%
- Power kW-meter: ±10% and ±20%

Fault detection thresholds are illustrated in FIGs. 18 - 24. Two types of horizontal lines are used in defining these thresholds. The *no-fault* line represents no flow rate reduction (or increase), no fouling and no inefficiencies in either the compressor or the motor. The *critical* line was determined by the following 3-step procedure:

1. Locate the points where the uncertainty boundaries intersect the no-fault line.

2. Project these points vertically to the points that intersect the 0.0°F curve (shown as black dots; for ±0.3 °F, refer to FIG. 18).

3 Draw horizontal lines, parallel to the abscissa, through these intersection points.

These horizontal lines are the critical lines and they define a region (shown as hatched in FIG. 18) within which it is possible for faults to go undetected. Beyond these critical lines (or thresholds), however, faults may be detected with more confidence despite the errors present in the measurement sensors.

For example, water flow rate abnormalities (reduction or increase) are detected most effectively by deviations in the conductance-area product and the entering/leaving water temperature difference of the given heat exchanger (evaporator or condenser). FIG. 18 shows the sensitivity of *UA* when used to detect flow rate reductions. The heavy solid curve represents the *UA* deviation in the face of no errors in the temperature and flow sensors (i.e., 0.0°F/0% of full scale, gpm). The dashed

and light solid curves represent the *UA* deviation due to errors of ±0.3°F/±5% gpm and ±0.6°F/±5% gpm, respectively.

Here, the critical lines are drawn using the uncertainty boundaries defined by ±0.6°F/±5% gpm. Based on a ±0.6°F/±5% gpm precision of these sensors, it can be concluded that *UA* deviations between −23.6% and +23.6% would not indicate a fault. Flow rate reductions greater than 41.0% and flow rate increases greater than 68.0% would be needed to indicate faults.

FIG. 19 is similar to FIG. 18 in terms of the precision errors represented by the heavy, dashed and light curves. However, the characteristic quantity used here is the entering/leaving water temperature difference instead of the conductance-area product. It is apparent from the critical lines drawn in FIG. 19 that the thresholds for detecting flow rate reduction is lower than those depicted in FIG. 18. In others words, this characteristic quantity has a greater fault detection sensitivity.

Quantitatively, here, it is concluded that water temperature difference deviations beyond −14.3% and +14.3% are used to detect flow rate increases greater than 16.0% and flow rate reductions greater than 13.0%, respectively.

Fouling describes a decrease in the effectiveness of the heat exchanger tubes, and is detected most effectively by deviations in the conductance-area product and the approach of the given device. FIG. 20 shows the sensitivity of *UA* when used to detect fouling. A fouling factor of 1 represents no fault and in this study, is the normalized equivalent of 0.00075 hr-ft^2/BTU. A factor greater than 1 is an increase

in fouling and lesser than 1 is a decrease. The critical lines indicate that UA deviations beyond −19.6% and +19.6% are used to detect fouling factors greater than 1.6 and lesser than 0.3, respectively.

FIG. 21 shows the sensitivity of the Approach when used to detect fouling. The critical lines indicates that *APPR* deviations beyond −17.6% and +17.6% are used to detect fouling factors lesser than 0.7 and greater than 1.3, respectively. These numbers, compared to those for *UA*, suggest that the *APPR* has lower fouling detection thresholds.

Some internal faults of the compressor are detected most effectively by deviations in its isentropic efficiency, $h_{isentropic}$. FIG. 22 shows the sensitivity of $\eta_{isentropic}$ when used to detect faults. A compressor fault factor of one represents no fault. In contrast to the fouling factor, a compressor fault factor greater than one is an improvement of the fault condition and a factor lesser than one is a worsening of the situation. The critical lines indicate that $\eta_{isentropic}$ deviations beyond −2.1% and +2.1% are used to detect fault factors lesser than 0.8 and greater than 1.2 respectively.

Deviations in the motor efficiency, η_{motor}, are used to detect faults in the motor or transmission housing. FIG. 23 shows the sensitivity of η_{motor} when detecting motor or transmission faults. The heavy solid curve represents the η_{motor} deviation when the kW-meter is error free (i.e., 0% of full scale, kW). The dashed and light solid curves represent the η_{motor} deviation due to errors of ±10% kW and ±20% kW,

respectively. A motor fault factor of one represents no fault and in this study, is equivalent to 0.85. However, factors greater than one represent worsening conditions.

Here, the critical lines are drawn using the uncertainty boundaries defined by the ±20% kW error. Based on this kW-meter precision, it is concluded that η_{motor} deviations less than –20% is used to detect fault factors greater than 1.3.

Equations (27)-(29) below are similar in form to the previous three relations for the condenser, and are used to model the chilled water reduction. Here, the chilled water flow rate reduction causes an increase in the return temperature and a decrease in the evaporator temperature for a given load and chilled water set point temperature.

$$\dot{m}_{chw,fault} = \dot{m}_{chw}\left(1-\frac{factor_{me}}{100}\right) \qquad (27)$$

$$\dot{Q}_{evap} = \dot{m}_{chw,fault}\, C_{pw}(T_{chwr}-T_{chws}) \qquad (28)$$

$$h_{ei} = 137\cdot\left(\frac{NEPASS\cdot \dot{m}_{chw,fault}}{NETUBE}\right)^{0.8}\cdot D_e^{-1.8} \qquad (29)$$

where, $\dot{m}_{chw,fault}$, $factor_{me}$, $NEPASS$, $NETUBE$ and D_e are the chilled water flow due to the flow reduction fault, the percentage reduction in chilled water flow rate, the number of evaporator tube passes, the number of evaporator tubes and the diameter of the evaporator tubes, respectively.

The CQs UA_e, $APPR_e$ and $CHWTD$ show the most significant deviations from the no-fault base-case. The CQ relationships here are similar to those used for the condenser water reduction fault. $CHWTD$ is the most sensitive and its sensitivity is unaffected by load changes.

Equations (30) and (31) are used to model condenser tube fouling. There are some conflicting interpretations of the fouling factor in the literature. Here, fouling is defined as the resistance to heat transfer due to the tube material as well as to any thin film build-up on its surfaces. Equation (30) is used to simulate an increase (or decrease) of the level of fouling in the condenser tubes. It is apparent from Equation (31) that as fouling increases, UA_c decreases.

$$R_{c,fault} = R_c \cdot factor_{fc} \qquad (30)$$

$$UA_c = \frac{A_{ci}}{\frac{1}{h_{c,i}} + \frac{1}{r_c h_{c,o}} + R_{c,fault}} \qquad (31)$$

where, $factor_{fc}$ is the fault modification factor used to simulate degrees of fouling in condenser (unity ≡ normal) and $R_{c,fault}$ is the resistance to heat transfer associated with the condenser tube material, including the fouling factor for faulty conditions.

The UA_c, and $APPR_c$ are CQs that show the more significant deviations from the no-fault base-case. FIG. 24 shows how these CQs deviate from the base-case condition as the fault condition changes (i.e., as fouling increases or decreases).

Similar to the flow reduction faults, the different CQs behave differently. For example, at a base-case load of 1500 tons, a 100% fouling increase by the condenser tubes corresponds to a 27% decrease and a 54% increase in UA_c and $APPR_c$, respectively. However, in contrast to condenser flow reduction faults, *CWTD* shows no significant change. This behavior is important in distinguishing the fouling fault from the flow reduction fault.

At 500 tons, the same fouling condition corresponds to a 29% decrease and 63% increase in UA_c and $APPR_c$, respectively. It is apparent from these results that the more sensitive CQ is the $APPR_c$ and that varying loading conditions affect it more than they did UA_c.

Similar trends exist for a 50% fouling decrease condition. CQs that increased before decreased and vise-verse. Fouling decrease information is as useful as fouling increase information. Here, FDD may be used to check the integrity of scheduled maintenance, repair or cleaning of fouled tubes.

Equations (32) and (33) are used to model evaporator tube fouling.

$$R_{e,fault} = R_e \cdot factor_{fe} \tag{32}$$

$$UA_e = \frac{A_{ei}}{\frac{1}{h_{e,i}} + \frac{1}{r_e h_{e,o}} + R_{e,fault}} \tag{33}$$

where, $factor_{fe}$, is the fault modification factor used to simulate degrees of fouling in the condenser (unity ≡ normal) and R_e and $R_{e,fault}$ are the resistance to heat transfer associated with the evaporator tube material, including the fouling factor for normal and for faulty conditions, respectively.

The UA_e and $APPR_e$ are CQs that show the more significant deviations from the no-fault base-case. The CQ relationships here are similar to those used for the condenser tube fouling fault. $APPR_e$ is more sensitive and its sensitivity is slightly affected by load changes.

The Weisner correlation, based on the measured performance of centrifugal compressors, is used for modeling compressor internal faults. The modification of the reference polytropic efficiency, η_{refer}, in Equation (34) is used to simulate possible faulty conditions within the compressor.

$$\eta_{refer,fault} = \eta_{refer} \cdot factor_{comp} \qquad (34)$$

where, $factor_{comp}$ and $\eta_{refer,fault}$, are the compressor fault modification factor, and the modified η_{refer} due to faulty conditions, respectively.

The compressor isentropic efficiency, $\eta_{isentropic}$ is the CQ that shows the most significant deviations from the no-fault base-case. FIG. 25 illustrates a greater decrease in the isentropic efficiency as the compressor fault factor decreases. Based on the manner in which this fault is simulated, a decrease in the fault factor means a

worsening compressor internal fault condition. Varying the loading conditions does not appear to have a great impact on the deviation of the isentropic efficiency.

Whenever there is a fault in the motor or transmission system of the compressor, the overall power draw (P) is expected to increase compared to the actual power used for the compression process. The modification factor in Equation (35) simulates this increase. Equation (35) defines the combined efficiency of the motor and transmission. An energy balance on the compressor establishes the relation between the states of the refrigerant at the suction and discharge conditions.

$$P_{fault} = P \cdot factor_{motor} \qquad (35)$$

$$\eta_{motor} = \frac{\dot{m}_{ref} \Delta h_{comp}}{P_{fault}}. \qquad (36)$$

where, P_{fault}, $factor_{motor}$ and $\Delta\eta_{comp}$ are the compressor power consumption due to faulty conditions, the motor fault modification factor and the change in refrigerant enthalpy between compressor's suction and discharge states, respectively.

The motor efficiency is the CQ that shows the most significant deviation from the no-fault base-case. FIG. 26 shows that there is a greater decrease in the motor efficiency as the motor fault factor increases (i.e., as the power draw increases for a given loading condition). From this simulation, the motor efficiency deviation (not the motor efficiency) is independent of loading conditions. That is, at

any loading condition, the percentage deviations due to an increased fault condition will show the same magnitudes.

Refrigerant loss results from leakage in chiller subsystems, which has the net effect of reducing overall system performance. It is often confirmed by bubbles present in the refrigerant (as seen from the liquid line sight glass), frost formation, abnormal superheat and subcooling temperatures, and abnormal unit operating pressures. A temperature difference between the low pressure liquid line temperature (entering the evaporator) and the suction line temperature (entering the compressor) was computed and used as a characteristic quantity to flag the occurrence of refrigerant leaks.

FIG. 27 summarizes the diagnostic patterns exhibited by the CQs discussed earlier. The symbols "⌀", "+" and "-" signify no significant change, an increase and a decrease compared to base-case values, respectively. In the *Type* column, "N", "F" and "N/A" stands for *Normal*, *Fault* and *Not Applicable*, respectively. Two normal operating conditions called "Load change" and "Heat-rejection change" are included. Respectively, these are quantities representing a change in the chiller load and a change in the amount of heat rejected by the condenser. They are modeled by varying the chilled water return and condenser water supply temperatures, respectively. These conditions are included to show that it is possible to distinguish them from fault conditions using the appropriate set of CQs.

Although, these CQs effectively isolate faults on the component level, the diagnostic patterns help to further distinguish between the various fault conditions that may exist in a particular component. For example, the increase and decrease in the condenser approach, $APPR_c$ and the condenser conductance-area product, UA_c, respectively, would signify that there is a problem in the condenser and not in the other components of the chiller sub-system. However, this same CQ change pattern is both exhibited by an increase in condenser tube fouling and a decrease in the condenser water flow rate. To distinguish between these two conditions, FIG. 27 shows that the condenser water flow rate decrease is accompanied by an increase in the condenser water temperature difference, $CWTD$, whereas the condenser tube fouling is not.

For most performance monitoring studies, the $COP_{overall}$ is a CQ that is often used to determine significant performance changes. The $COP_{overall}$ is included in FIG. 27 to illustrate that although it gives some indication of changes within a chiller sub-system, by itself, it is quite vague in isolating faulty components or in diagnosing faults within a given component. Therefore, it must be used in combination with the other CQs, mentioned here, for useful diagnoses to be made.

According to one modification of the above-described FDD methodology, the use of a base-case lookup table is eliminated. Notably, the use of parallel fault detection and diagnosis in which CQ residuals are derived from comparing a particular chiller to other identical (similar model, capacity and run-time)

chillers within the same HVAC system eliminates the need for a lookup table. In parallel FDD, the data from a designated chiller is considered to be the base-case, and faults are detected by comparing the data from another chiller with the data from the designated chiller. In so doing, faults in a particular chiller or chillers are determined over a predetermined time period.

The parallel FDD methodology is substantially similar to the above described (serial) FDD methodology in all relevant respects. As will be appreciated by one of ordinary skill in the art, in parallel FDD the CQ's from the designated chiller and the other chiller(s) are determined on-the-fly, and the difference (residuals) between the two streams of CQ's is used to detect faults in the previously described manner.

One of ordinary skill in the art will appreciate that both of the above-described embodiments of the present invention utilize CQ's and thus do not require modification or tuning of the thermodynamic model. Accordingly, the FDD system of the present invention may readily be included in an existing facility management system, provided that the appropriate sensors are already installed. Use of the first embodiment merely requires the collection and storing of base-case CQ's whereas base-case CQ's are calculated on the fly according to parallel FDD.

Another benefit of the present invention relates to threshold used to detect the occurrence of faults. Both of the above-described embodiments detect of faults by comparing operating CQ's to base-case CQ's. A fault is detected when one

or more CQ's exceed a predetermined threshold which is determined in relation to the sensor accuracy. Accordingly, the false detection of faults is minimized.

Yet another benefit of the claimed invention relates to the classification of faults. Notably, the inventor of the present invention discovered that certain CQ's are more sensitive than others to the occurrence of faults, and that faults may accurately be diagnosed by examination of which CQ's exceed the predetermined threshold.

While various embodiments of the present invention have been shown and described, it should be understood that other modifications, substitutions and alternatives are apparent to one of ordinary skill in the art. Such modifications, substitutions and alternatives can be made without departing from the spirit and scope of the invention, which should be determined from the appended claims.

Various features of the invention are set forth in the appended claims.

WHAT IS CLAIMED IS:

1. A fault detection system for an HVAC system including sensors for measuring the performance of one or more of a condenser, a compressor, an evaporator, and a chiller, said fault detection system comprising:

a processing means for generating characteristic quantities (CQ's) from a plurality of measured inputs;

means for storing plural CQ values generated by said processing means in an initial period in which fault-free operation of the HVAC system is assumed, CQ values being generated for each of plural different measured input values;

means for producing interpolated base-case CQ values from said plural stored CQ values for a given set of measured inputs;

means for detecting a fault when a difference between actual CQ values, calculated by said processing means using said given set of measured inputs, and said interpolated base-case CQ values varies from a predetermined threshold value;

means for classifying a detected fault based on which ones of said actual CQ values varies from said interpolated CQ values.

2. The fault detection system according to claim 1 wherein said processing means uses measured inputs selected from the group comprising: chilled water supply temperature; chilled water return temperature; condenser water supply temperature; chilled water flow rate; condenser water flow rate; evaporator saturation

temperature; condenser saturation temperature; and compressor discharge temperature.

3. The fault detection system according to claim 1 wherein said interpolator is a General Regression Neural Network.

4. The fault detection system according to claim 1 wherein said interpolator is a Probabilistic Neural Network.

5. The fault detection system according to claim 1 wherein said interpolator is a Back Propagation Network.

6. The fault detection system according to claim 1 wherein said CQ's are selected from the group comprising: evaporator heat exchanger approach; condenser heat exchanger approach; chilled water temperature difference; condenser water temperature; condenser conductance-area product; condenser conductance-area product; isentropic efficiency; motor/transmission efficiency; overall coefficient of performance; and compressor coefficient of performance.

7. The fault detection system according to claim 6 wherein condenser water flow rate abnormalities are diagnosed when one of said condenser conductance-

area product, said condenser heat exchanger approach, and said condenser water temperature difference exceeds said predetermined threshold value for said CQ.

8. The fault detection system according to claim 6 wherein chilled water flow rate abnormalities are diagnosed when one of said evaporator conductance-area product, said evaporator heat exchanger approach, and said chilled water temperature difference exceeds said predetermined threshold value for said CQ.

9. The fault detection system according to claim 6 wherein chilled water flow rate abnormalities are diagnosed when one of said evaporator conductance-area product, said evaporator heat exchanger approach, and said chilled water temperature difference exceeds said predetermined threshold value for said CQ.

10. The fault detection system according to claim 6 wherein evaporator tube fouling is diagnosed when one of said evaporator conductance-area product and said evaporator heat exchanger approach exceeds said predetermined threshold value for said CQ.

11. The fault detection system according to claim 6 wherein condenser tube fouling is diagnosed when one of said condenser conductance-area product and said

condenser heat exchanger approach exceeds said predetermined threshold value for said CQ.

12. The fault detection system according to claim 6 wherein an internal compressor internal fault is diagnosed when one of said compressor coefficient of performance, said isentropic efficiency, and compressor power draw exceeds said predetermined threshold value for said CQ.

13. The fault detection system according to claim 6 wherein a motor transmission fault is diagnosed when one of said overall coefficient of performance, said motor/transmission efficiency, and motor power draw exceeds said predetermined threshold value for said CQ.

14. The fault detection system according to claim 6 wherein said predetermined threshold includes upper and lower critical value levels for each said characteristic quantity, said upper and lower critical value levels being determined in accordance with a rated precision error of a sensor used to acquire a selected said measured input used to calculate said characteristic quantities.

15. A method for detecting faults in a chiller subsystem of a facility cooling system, comprising:

providing plural base data sets of measured inputs, each said set of measured inputs including sensor data for a different base operating condition of the chiller;

computing a set of characteristic quantities for each of said plural base data sets;

storing said plural sets of characteristic quantities in a memory means;

providing a test data set for a test operating condition of the chiller;

computing a set of characteristic quantities from said test data set;

producing an interpolated base set of characteristic quantities from among said plural sets of characteristic quantities stored in said memory means using said test data set;

detecting a fault when at least one characteristic quantity exceeds a predetermined threshold range;

diagnosing a fault in relation to which ones of said characteristic quantities exceed said predetermined threshold range.

16. The method according to claim 15 wherein said predetermined threshold range includes upper and lower critical value levels for each said characteristic quantity, said upper and lower critical value levels being determined in accordance with a rated precision error of a sensor used to acquire data items contained in said test data set.

17. The method according to claim 15 wherein said measured inputs are selected from the group comprising: {chilled water supply temperature; chilled water return temperature; condenser water supply temperature; chilled water flow rate; condenser water flow rate; evaporator saturation temperature; condenser saturation temperature; and compressor discharge temperature.

18. The method according to claim 15 wherein said characteristic quantities are selected from the group comprising: evaporator heat exchanger approach; condenser heat exchanger approach; chilled water temperature difference; condenser water temperature; condenser conductance-area product; condenser conductance-area product; isentropic efficiency; motor/transmission efficiency; overall coefficient of performance; and compressor coefficient of performance.

19. The method according to claim 18 wherein condenser water flow rate abnormalities are diagnosed when one of said condenser conductance-area product, said condenser heat exchanger approach, and said condenser water temperature difference exceeds said predetermined threshold value for said CQ.

20. The method according to claim 18 wherein chilled water flow rate abnormalities are diagnosed when one of said evaporator conductance-area product,

said evaporator heat exchanger approach, and said chilled water temperature difference exceeds said predetermined threshold value for said CQ.

21. The method according to claim 18 wherein water flow rate abnormalities in said chilled water flow are detected when one of said evaporator conductance-area product, said evaporator heat exchanger approach, and said chilled water temperature difference exceeds said predetermined threshold value for said CQ.

22. The method according to claim 18 wherein evaporator tube fouling is diagnosed when one of said evaporator conductance-area product and said evaporator heat exchanger approach exceeds said predetermined threshold value for said CQ.

23. The method according to claim 18 wherein condenser tube fouling is diagnosed when one of said condenser conductance-area product and said condenser heat exchanger approach exceeds said predetermined threshold value for said CQ.

24. The method according to claim 18 wherein an internal compressor internal fault is diagnosed when one of said compressor coefficient of performance, said isentropic efficiency, and compressor power draw exceeds said predetermined threshold value for said CQ.

25. The method according to claim 18 wherein a motor transmission fault is diagnosed when one of said overall coefficient of performance, said motor/transmission efficiency, and motor power draw exceeds said predetermined threshold value for said CQ.

26. A fault detection and diagnosis system for a HVAC system including at least two chillers, each chiller being equipped with sensors for measuring the performance of one or more condenser, a compressor, an evaporator, and a chiller, said fault detection system comprising:

processing means for calculating characteristic quantities (CQ's) from a plurality of measured inputs for each of the chillers, one chiller being designated as a base-case chiller;

means for detecting a fault when a difference between CQ values for the base case chiller and CQ values for other ones of the chillers exceeds a predetermined threshold range for at least one of said CQ values;

a fault classifier for classifying a detected fault based on which ones of said actual CQ values exceed said threshold range.

27. The fault detection system according to claim 26 wherein said CQ's are selected from the group comprising: evaporator heat exchanger approach; condenser heat exchanger approach; chilled water temperature difference; condenser water

temperature; condenser conductance-area product; condenser conductance-area product; isentropic efficiency; motor/transmission efficiency; overall coefficient of performance; and compressor coefficient of performance.

28. The fault detection system according to claim 27 wherein condenser water flow rate abnormalities are diagnosed when one of said condenser conductance-area product, said condenser heat exchanger approach, and said condenser water temperature difference exceeds said predetermined threshold value for said CQ.

29. The fault detection system according to claim 27 wherein chilled water flow rate abnormalities are diagnosed when one of said evaporator conductance-area product, said evaporator heat exchanger approach, and said chilled water temperature difference exceeds said predetermined threshold value for said CQ.

30. The fault detection system according to claim 27 wherein chilled water flow rate abnormalities are diagnosed when one of said evaporator conductance-area product, said evaporator heat exchanger approach, and said chilled water temperature difference exceeds said predetermined threshold value for said CQ.

31. The fault detection system according to claim 27 wherein evaporator tube fouling is diagnosed when one of said evaporator conductance-area product and

said evaporator heat exchanger approach exceeds said predetermined threshold value for said CQ.

32. The fault detection system according to claim 27 wherein condenser tube fouling is diagnosed when one of said condenser conductance-area product and said condenser heat exchanger approach exceeds said predetermined threshold value for said CQ.

33. The fault detection system according to claim 27 wherein an internal compressor internal fault is diagnosed when one of said compressor coefficient of performance, said isentropic efficiency, and compressor power draw exceeds said predetermined threshold value for said CQ.

34. The fault detection system according to claim 27 wherein a motor transmission fault is diagnosed when one of said overall coefficient of performance, said motor/transmission efficiency, and motor power draw exceeds said predetermined threshold value for said CQ.

35. The method according to claim 27 wherein said predetermined threshold includes upper and lower critical value levels for each said characteristic quantity, said upper and lower critical value levels being determined in accordance

with a rated precision error of a sensor used to acquire a selected said measured input used to calculate said characteristic quantities.

36. The fault detection system according to claim 26 further comprising:

means for producing interpolated base-case CQ values from base-case chiller for a given set of measured inputs;

wherein said fault detecting means detects a fault when a difference between said interpolated base-case CQ values and CQ values for other ones of the chillers exceeds a predetermined threshold range for at least one of said CQ values.

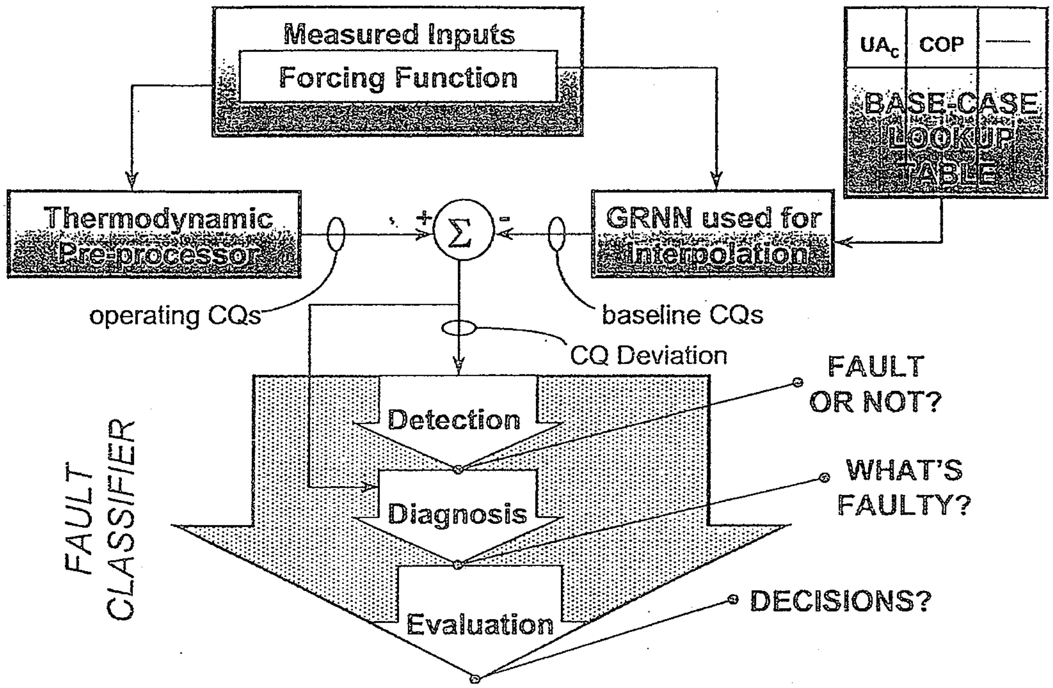
Measured Inputs
Forcing Function
UA$_c$
COP
BASE-CASE LOOKUP TABLE
Thermodynamic Pre-processor
GRNN used for interpolation
+
-
operating CQs
baseline CQs
CQ Deviation
Detection
Diagnosis
Evaluation
FAULT CLASSIFIER
FAULT OR NOT?
WHAT'S FAULTY?
DECISIONS?

FIG. 1

FIG. 2

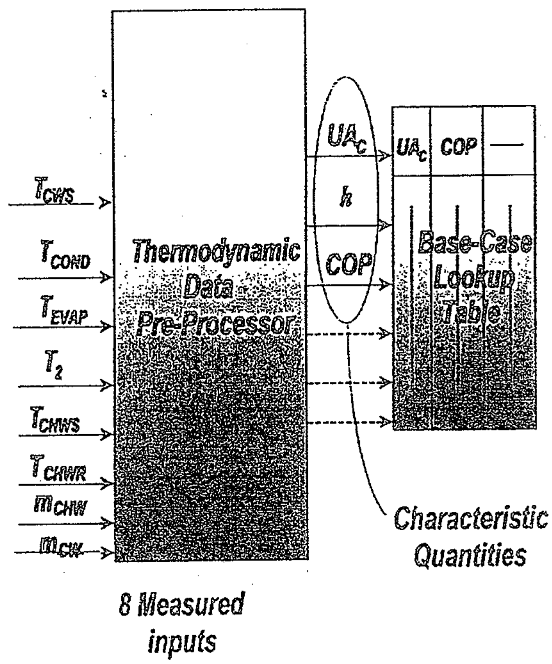
T_{CWS}
T_{COND}
T_{EVAP}
T_2
T_{CHWS}
T_{CHWR}
m_{CHW}
m_{CW}
Thermodynamic Data Pre-Processor
UA_C
h
COP
UA_C
COP
Base-Case Lookup Table
Characteristic Quantities
8 Measured inputs

FIG. 3

```
Procedure LMTDe_(T_chws,T_chwr,T_evap:LMTDe,T_we,ln_arg_e)

T_we = (T_chws +T_chwr)/2

ln_arg_e = max(0,(T_chwr-T_evap)/(T_chws-T_evap))

If ((T_chws = T_chwr) OR (ln_arg_e=0)) Then

LMTDe = T_we - T_evap

Else

    If (T_evap > T_chws) Then Call Error

    If (T_chws > T_chwr) Then Call Error

    LMTDe_real = ((T_chwr-T_evap)-(T_chws-T_evap))/ln(ln_arg_e)

    LMTDe = max(0,LMTDe_real)

EndIf

End
```

FIG. 4

```
Procedure LMTD_c(T_cws,T_cwr,T_cond:LMTDc,T_wc,ln_arg_c)

T_wc = (T_cws + T_cwr)/2

ln_arg_c = max(0,(T_cond-T_cws)/(T_cond-T_cwr))

If (T_cwr = T_cws) OR (ln_arg_c =0) Then

LMTDc = T_cond - T_wc

Else

        If (T_cond < T_cwr) Then Call Error

If (T_cwr < T_cws) Then Call Error

        LMTDc_real = ((T_cond-T_cws)-(T_cond-T_cwr)) / ln(ln_arg_c)

        LMTDc = max(0,LMTDc_real)

EndIf

End
```

FIG. 5

time = tablerun#

T_cws = lookup(time, #T_cws) "F"

Gpmcw = lookup(time, #Gpmcw) "gpm"

T_cond = lookup(time, #T_cond) "F"

FIG. 6

T_chws = lookup(time, #T_chws) "F"

T_chwr = lookup(time, #T_chwr)"F"

Gpmchw = lookup(time, #Gpmchw) "gpm"

T_evap = lookup(time, #T_evap) "F"

FIG. 7

T_2 = lookup(time, #T_2) "F"

Power = lookup(time, #Power) "kW"

FIG. 8

Q_evap = Gpmchw * ft3hr\gpm * dens_chw * Cpw * (T_chwr - T_chws)/12000 "ton"

Q_evap = UAe * LMTDe /12000 "ton"

Q_evap = Gpm_R * ft3hr\gpm * dens_R* (h_1 - h_4)/12000 "ton"

h_1 = Enthalpy(R22, x = 1, P = P_evap) "Btu/lbm"

v_1 = Volume(R22, x = 1, T = T_evap) "ft^3/lbm"

T_evap = Temperature(R22,x = 0,P = P_evap) "F"

APPRe = T_chws - T_evap "F"

CHWTD = T_chwr - T_chws "F"

FIG. 9

```
P_comp = Gpm_R * ft3hr\gpm * dens_R * (h_2 - h_1)/12000 * kW\ton "kW"

P_comp = P_ideal/eta "kW"

P_ideal = Gpm_R * ft3hr\gpm * dens_R * (h_2s - h_1)/12000 *kW\ton "kW"

s_1 = Entropy(R22, x = 1, P = P_evap) "Btu/lbm-R"

s_2s = s_1 "Btu/lbm-R"

h_2s = Enthalpy(R22, s = s_2s, P = P_cond) "Btu/lbm"

COP_overall = Q_evap /(Power / kW\ton)

COP_comp = Q_evap /(P_comp / kW\ton)

COP_ideal = Q_evap /(P_ideal / kW\ton)

EFFMOT = P_comp/Power

P_ratio = P_cond/P_evap
```

FIG. 10

"CONDENSER EQUATIONS:"

Q_cond = Gpmcw * ft3hr\gpm * dens_cw * Cpw * (T_cwr - T_cws)/12000 "ton"

Q_cond = UAc * LMTDc /12000 "ton"

Q_cond = Gpm_R * ft3hr\gpm * dens_R * (h_2 - h_3)/12000 "ton"

h_3 = Enthalpy(R22, x = 0, P = P_cond) "Btu/lbm"

v_3 = Volume(R22, x = 0, P = P_cond) "ft^3/lbm"

T_cond = Temperature(R22, x = 0, P = P_cond) "F"

T_2 = Temperature(R22, h = h_2, P = P_cond) "F"

v_2 = Volume(R22, h = h_2, P = P_cond) "ft^3/lbm"

APPRc = T_cond - T_cwr "F"

CWTD = T_cwr - T_cws "F"

FIG. 11

"EXPANSION VALVE EQUATION:"

h_4 = h_3 "Btu/lbm"

FIG. 12

"PROPERTY & CONVERSION DATA:"

dens_chw = Density(Water, T=(T_chws+T_chwr)/2, P=14.7) "lbm/ft^3"

dens_cw = Density(Water, T=(T_cws+T_cwr)/2, P=14.7) "lbm/ft^3"

dens_R = Density(R22, T=(T_cond+T_evap)/2, P=(P_cond +P_evap)/2) "lbm/ft^3"

Cpw = 1.0 "Btu/lbm-R"

ft3hr\gpm = convert(gal,ft3)/convert(min,hr)

kW\ton = convert(ton,kW)

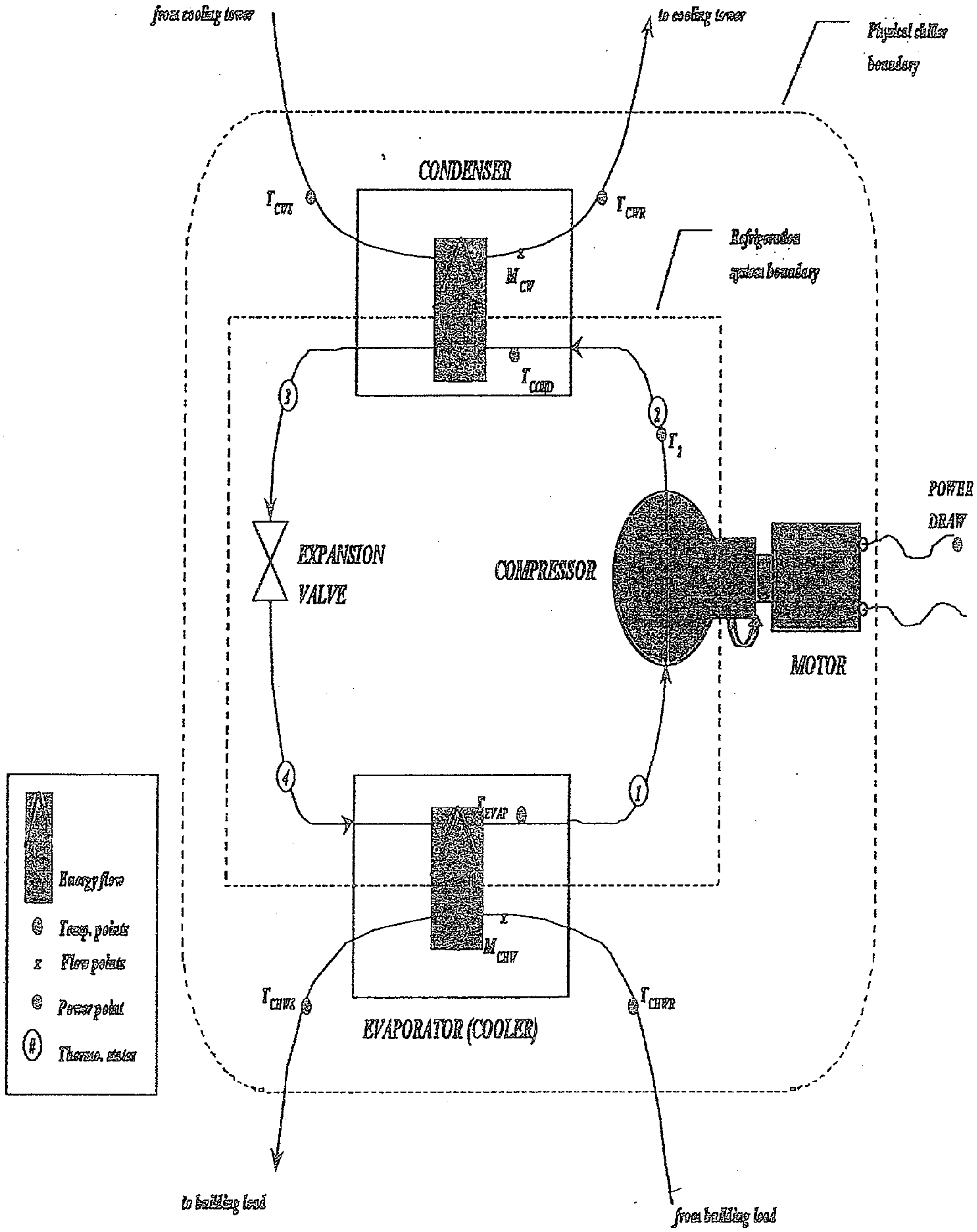

from cooling tower
to cooling tower
Physical chiller boundary
CONDENSER
T_{CWS}
T_{CWR}
Refrigeration system boundary
M_{CW}
T_{COND}
3
2
T_2
POWER DRAW
EXPANSION VALVE
COMPRESSOR
MOTOR
4
1
T_{EVAP}
Energy flow
Temp. points
x Flow points
Power point
Thermo. states
M_{CHW}
T_{CHWS}
T_{CHWR}
EVAPORATOR (COOLER)
to building load
from building load

FIG. 13

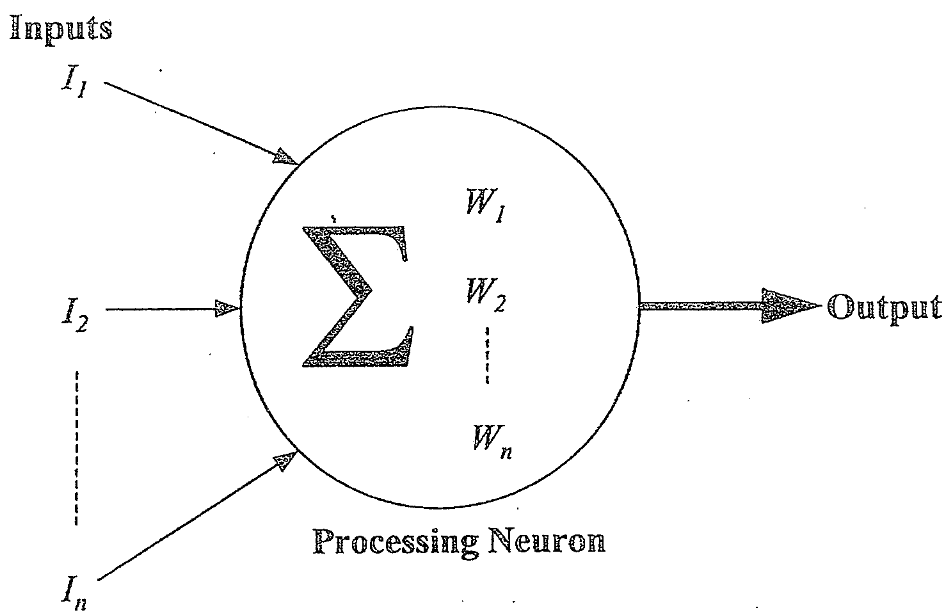

FIG. 14

FIG. 15

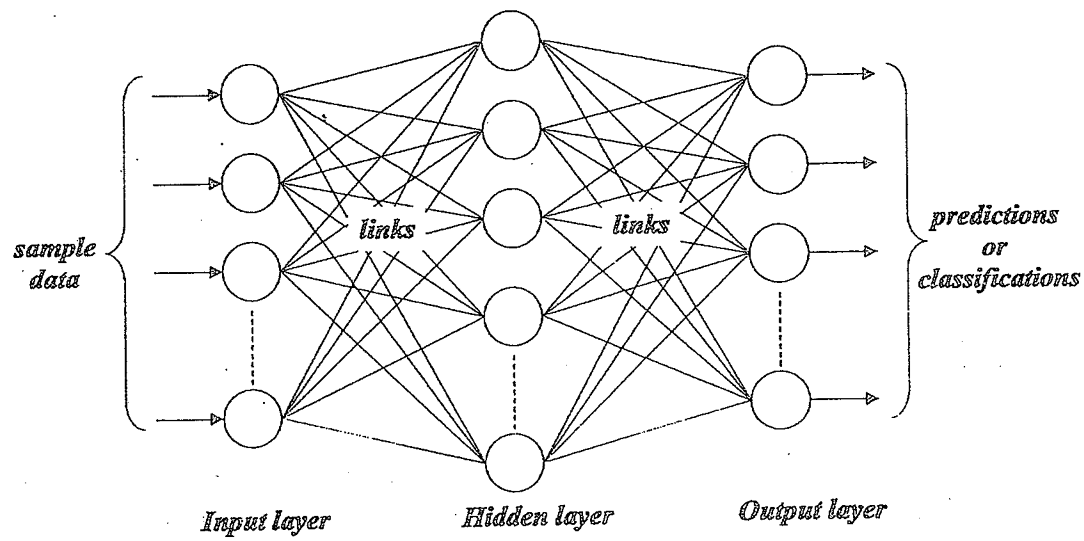
sample data
links
links
predictions or classifications
Input layer
Hidden layer
Output layer

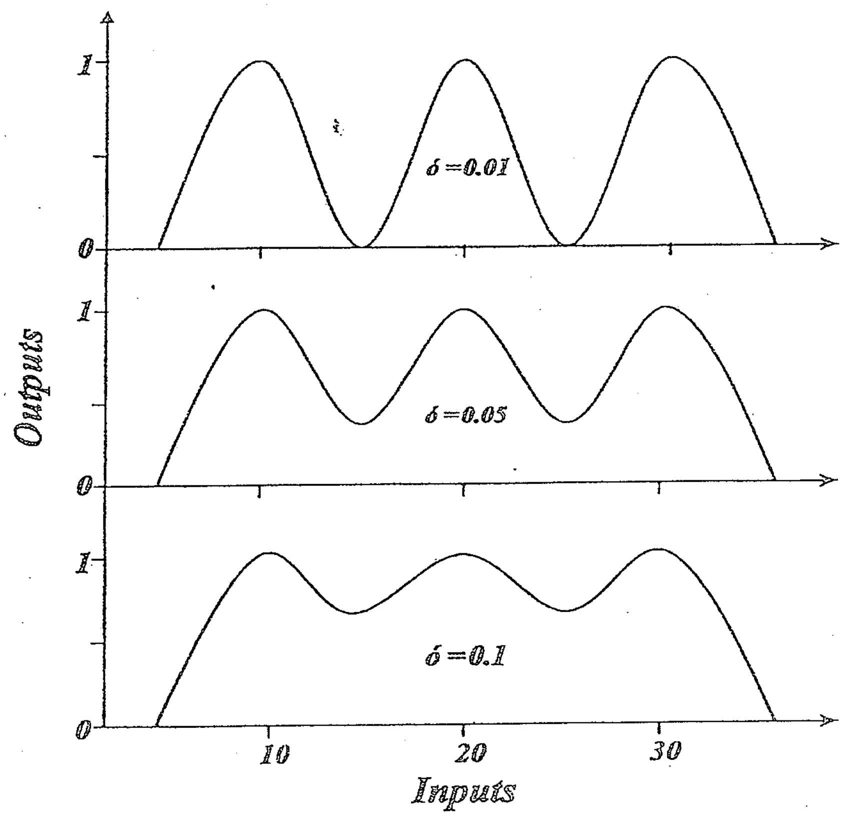

FIG. 16A

FIG. 16B

FIG. 16C

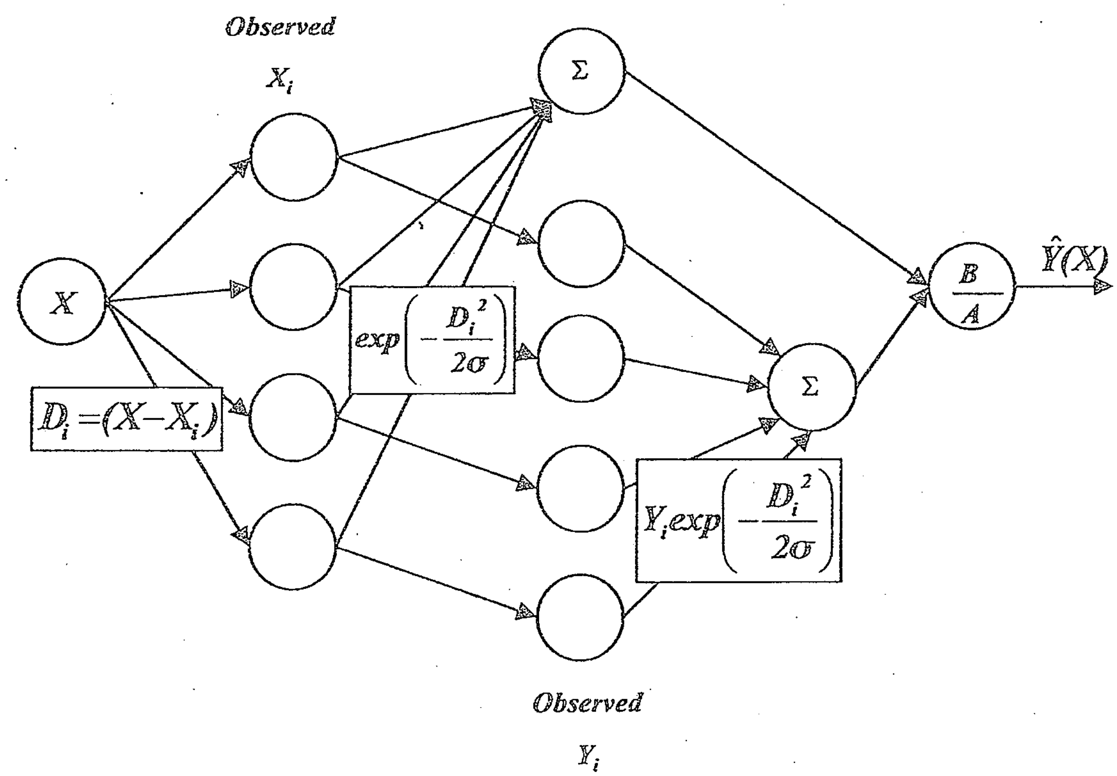
Observed
X_i
Σ
X
$D_i = (X - X_i)$
$exp\left(-\frac{D_i^2}{2\sigma}\right)$
Σ
$Y_i exp\left(-\frac{D_i^2}{2\sigma}\right)$
$\frac{B}{A}$
$\hat{Y}(X)$
Observed
Y_i

FIG. 17

FIG. 18

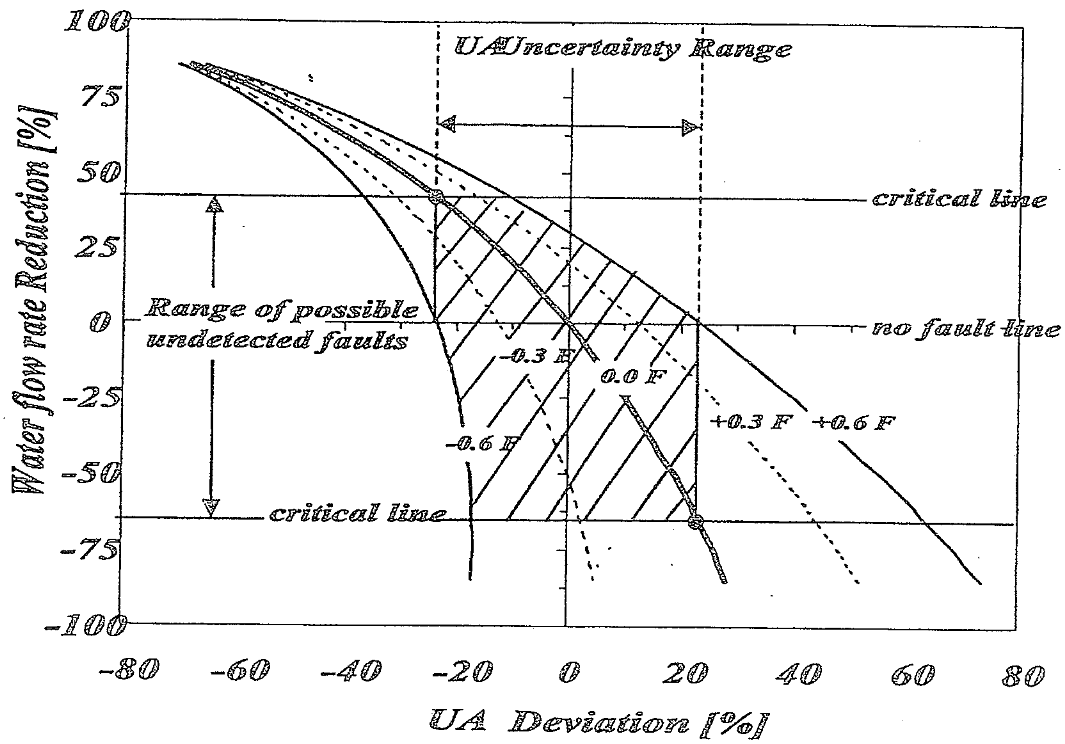
UA Uncertainty Range
critical line
no fault line
Range of possible
undetected faults
critical line
-0.3 F
0.0 F
+0.3 F
+0.6 F
-0.6 F
100
75
50
25
0
-25
-50
-75
-100
-80
-60
-40
-20
0
20
40
60
80
Water flow rate Reduction [%]
UA Deviation [%]

FIG. 19

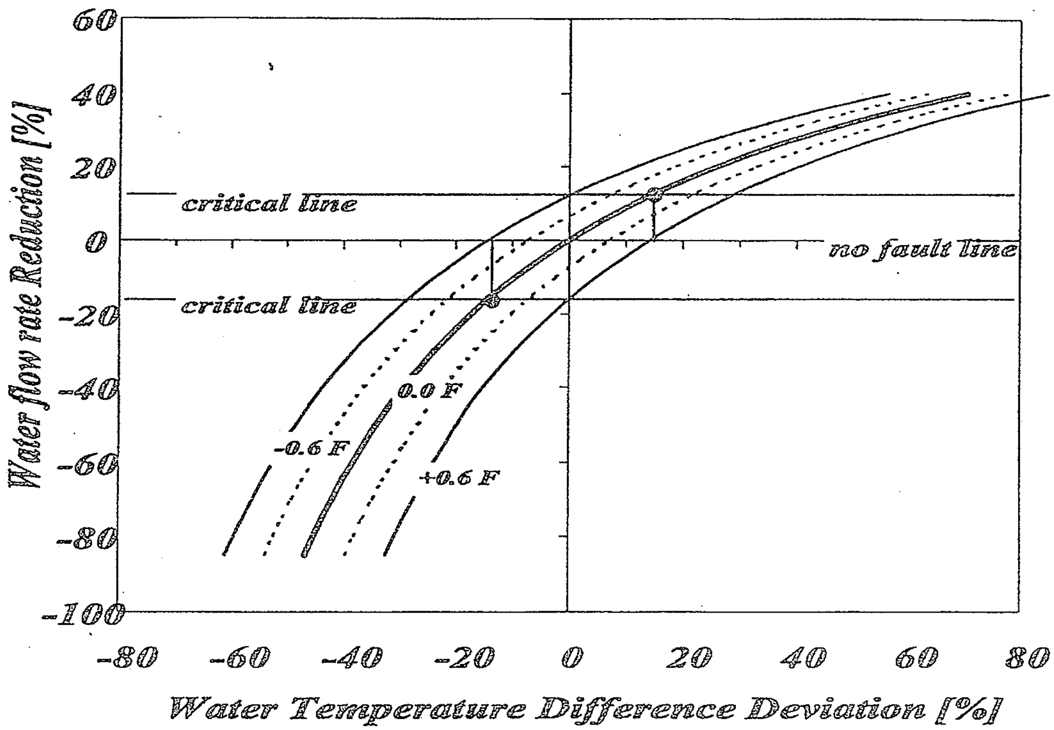
60
40
20
0
-20
-40
-60
-80
-100
-80
-60
-40
-20
0
20
40
60
80
Water flow rate Reduction [%]
Water Temperature Difference Deviation [%]
critical line
critical line
no fault line
-0.6 F
0.0 F
+0.6 F

FIG. 20

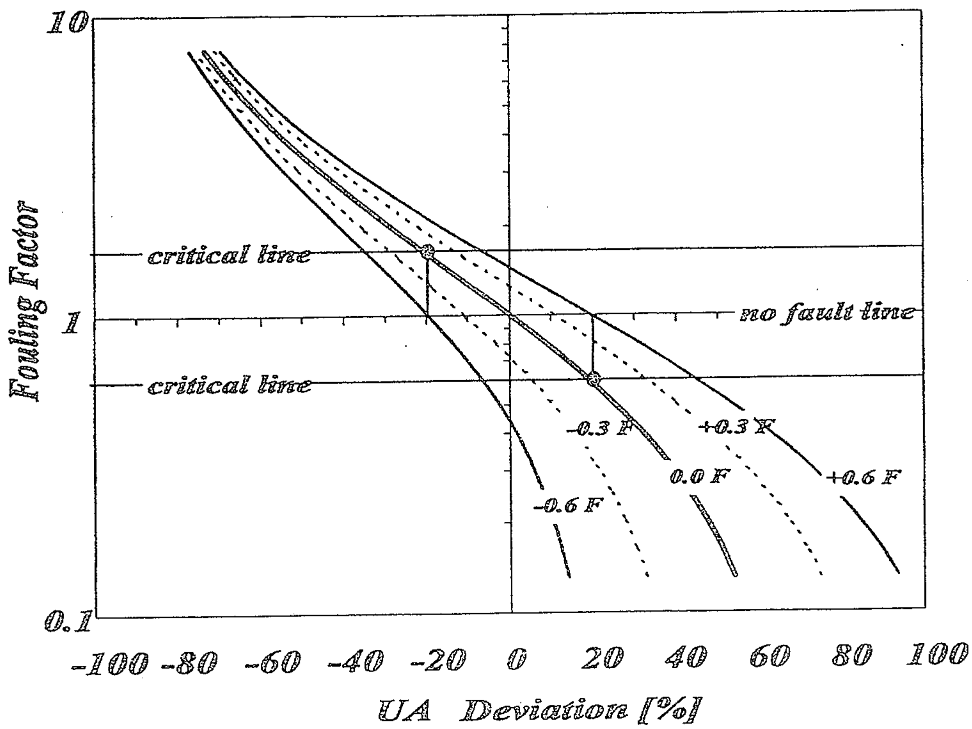
10
1
0.1
Fouling Factor
critical line
critical line
no fault line
-0.6 F
-0.3 F
0.0 F
+0.3 F
+0.6 F
-100
-80
-60
-40
-20
0
20
40
60
80
100
UA Deviation [%]

FIG. 21

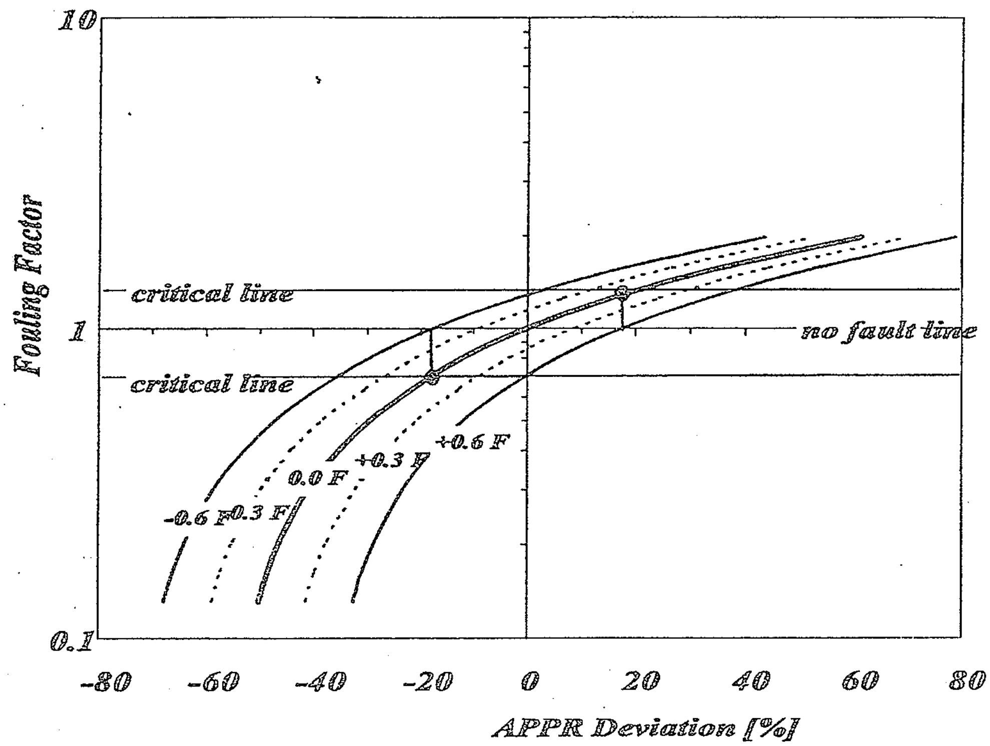
10
1
0.1
Fouling Factor
critical line
critical line
no fault line
-0.6 F
-0.3 F
0.0 F
+0.3 F
+0.6 F
-80
-60
-40
-20
0
20
40
60
80
APPR Deviation [%]

FIG. 22

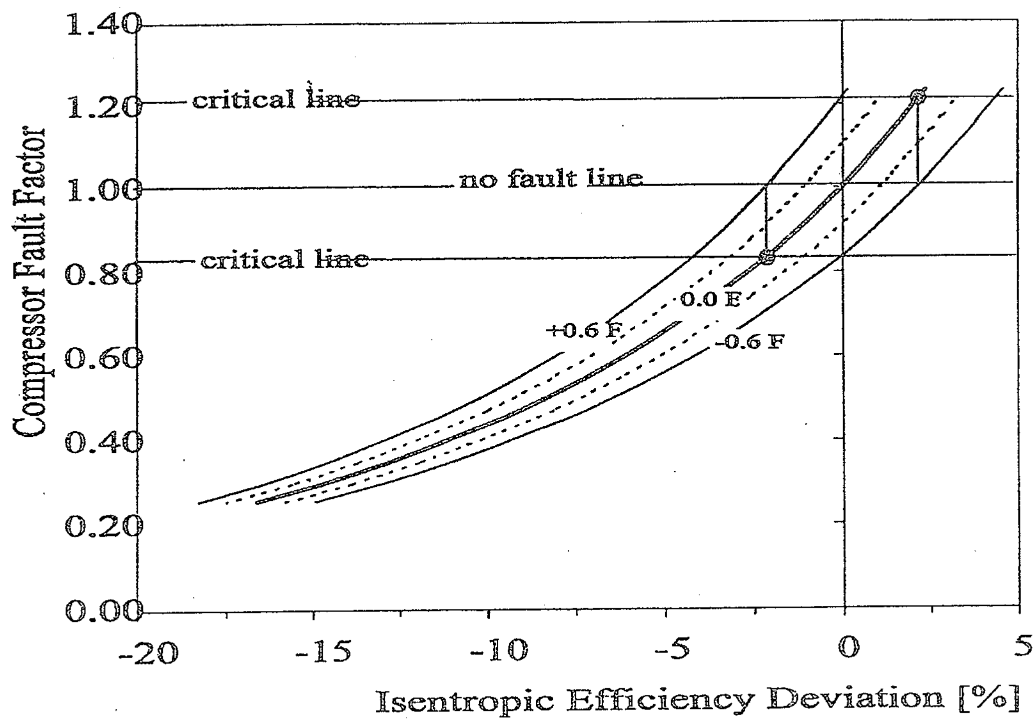
1.40
1.20
1.00
0.80
0.60
0.40
0.20
0.00
critical line
no fault line
critical line
+0.6 F
0.0 F
-0.6 F
Compressor Fault Factor
-20
-15
-10
-5
0
5
Isentropic Efficiency Deviation [%]

FIG. 23

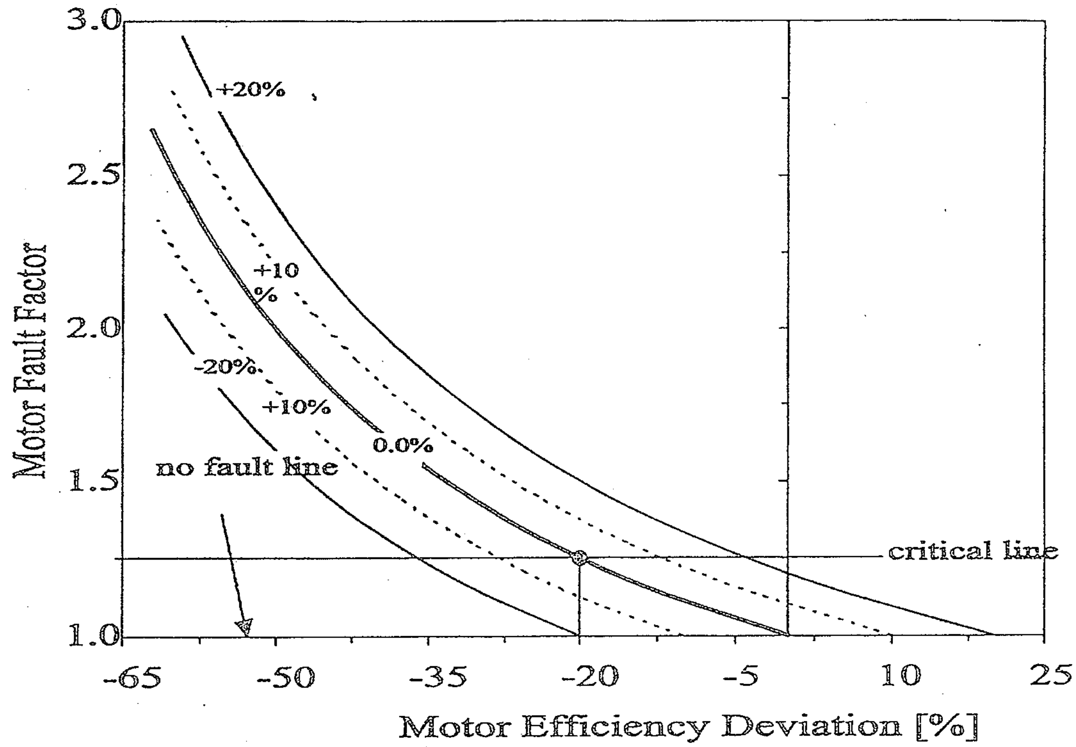
3.0
2.5
2.0
1.5
1.0
Motor Fault Factor
+20%
+10
%
-20%
+10%
0.0%
no fault line
critical line
-65
-50
-35
-20
-5
10
25
Motor Efficiency Deviation [%]

FIG. 24

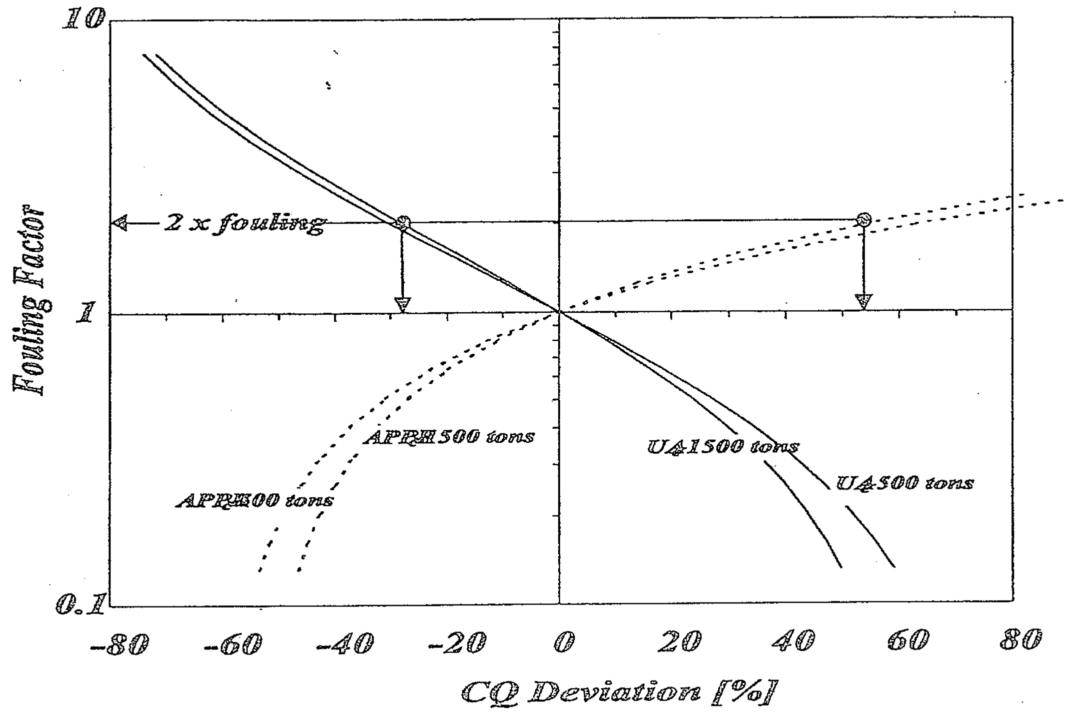
10
1
0.1
Fouling Factor
2 x fouling
APRH500 tons
APRH100 tons
UA1500 tons
UA500 tons
-80
-60
-40
-20
0
20
40
60
80
CQ Deviation [%]

FIG. 25

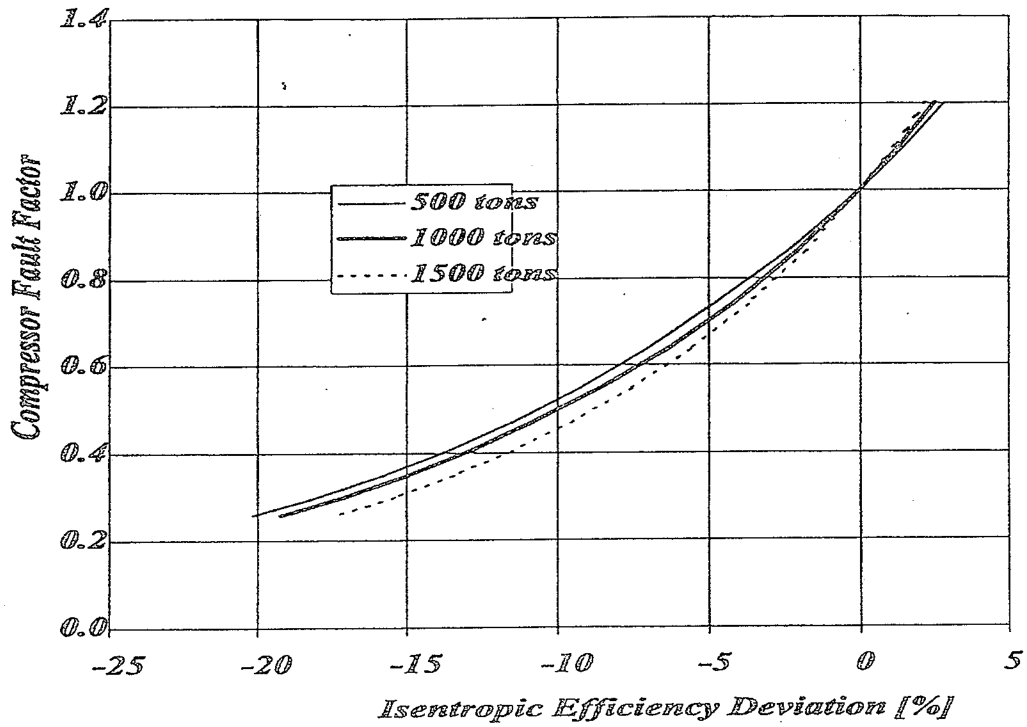

Compressor Fault Factor
1.4
1.2
1.0
0.8
0.6
0.4
0.2
0.0
500 tons
1000 tons
1500 tons
-25
-20
-15
-10
-5
0
5
Isentropic Efficiency Deviation [%]

FIG. 26

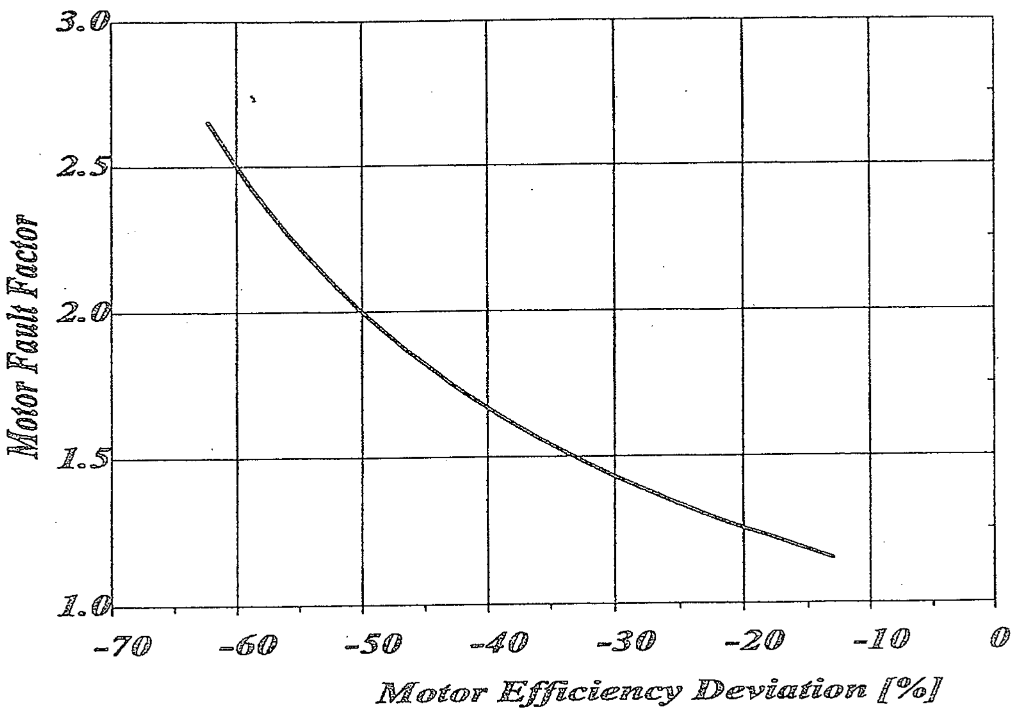
3.0
2.5
2.0
1.5
1.0
Motor Fault Factor
-70
-60
-50
-40
-30
-20
-10
0
Motor Efficiency Deviation [%]

FIG. 27

Operating Condition	Δ	Type	CQs used for FDD in a Chiller sub-system										
			Evaporator				*Condenser*				*Compressor*		*Chiller*
			Q_{evap}	*CHWTD*	$APPR_e$	UA_e	Q_{cond}	*CWTD*	$APPR_c$	UA_c	$\eta_{isentropic}$	η_{motor}	$COP_{overall}$
Base-Case	N/A	N	∅	∅	∅	∅	∅	∅	∅	∅	∅	∅	∅
Heat Rejection change	incr	N	∅	∅	∅	∅	+	∅	∅	∅	∅	∅	-
	decr	N	∅	∅	∅	∅	-	∅	∅	∅	∅	∅	+
Load change	incr	N	+	+	+	-	+	+	+	+	+	+	+
	decr	N	-	-	-	+	-	-	-	-	-	-	-
Chilled water Flow change	incr	F	∅	-	-	+	∅	∅	∅	∅	∅	∅	+
	decr	F	∅	+	+	-	∅	∅	∅	∅	∅	∅	-
Condenser water Flow change	incr	F	∅	∅	∅	∅	∅	-	-	+	∅	∅	+
	decr	F	∅	∅	∅	∅	∅	+	+	-	∅	∅	-
Evaporator tube Fouling	incr	F	∅	∅	+	-	∅	∅	∅	∅	∅	∅	-
	decr	N/A	∅	∅	-	+	∅	∅	∅	∅	∅	∅	+
Condenser tube Fouling	incr	F	∅	∅	∅	∅	∅	∅	+	-	∅	∅	-
	decr	N/A	∅	∅	∅	∅	∅	∅	-	+	∅	∅	+
Compressor Internal faults	incr	F	∅	∅	∅	∅	∅	∅	∅	∅	-	∅	-
Motor/Transmission Faults	incr	F	∅	∅	∅	∅	∅	∅	∅	∅	∅	-	-

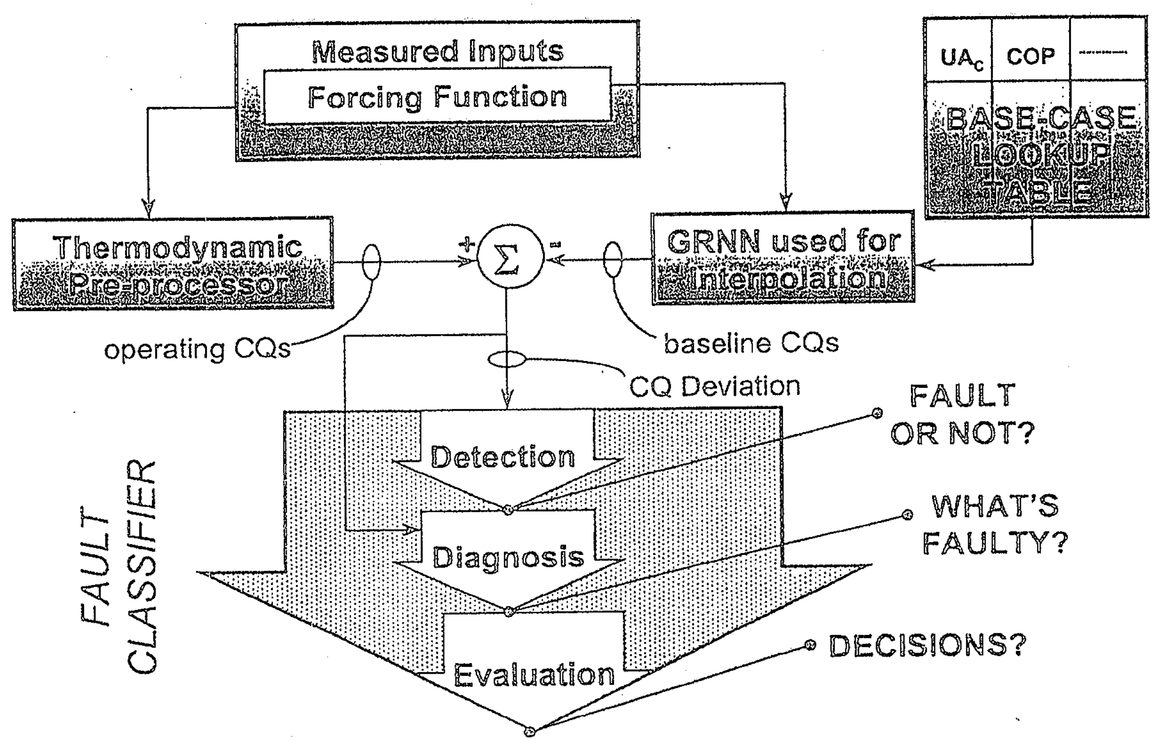

Measured Inputs
Forcing Function
UA_c
COP
BASE-CASE LOOKUP TABLE
Thermodynamic Pre-processor
GRNN used for interpolation
+
-
Σ
operating CQs
baseline CQs
CQ Deviation
FAULT CLASSIFIER
Detection
Diagnosis
Evaluation
FAULT OR NOT?
WHAT'S FAULTY?
DECISIONS?

DERWENT-ACC-NO: 2002-395124

DERWENT-WEEK: 200243

TITLE: Fault detection and diagnosis in HVAC sub-systems, uses a thermodynamic preprocessor for calculating characteristic quantities (CQ) from measured inputs, and base-case lookup table for CQ values from first fault-free operation period

INVENTOR: MCINTOSH I B D

PATENT-ASSIGNEE: SIEMENS BUILDING TECHNOLOGIES INC[SIEI]

PRIORITY-DATA: 2000US-619877 (July 20, 2000)

PATENT-FAMILY:

PUB-NO	PUB-DATE	LANGUAGE
CA 2344908 A1	January 20, 2002	EN

APPLICATION-DATA:

PUB-NO	APPL-DESCRIPTOR	APPL-NO	APPL-DATE
CA 2344908A1	N/A	2001CA-2344908	April 23, 2001

INT-CL-CURRENT:

TYPE	IPC DATE
CIPS	F24F11/02 20060101
CIPS	F25D29/00 20060101

ABSTRACTED-PUB-NO: CA 2344908 A1

BASIC-ABSTRACT:

NOVELTY - The fault detection system has sensors for measuring the performance of a condenser, a compressor, an evaporator, and a

chiller. The system has a thermodynamic preprocessor for calculating characteristic quantities (CQ's) from a plurality of measured inputs. Also provided is a base-case lookup table for storing plural first sets of CQ values generated by the thermodynamic preprocessor in an initial period in which fault-free operation of the HVAC system is assumed, a first set of CQ values being generated for each of plural different measured input values.

DESCRIPTION - An interpolator interpolates a set of base-case CQ values from the first sets of CQ values stored in the base-case lookup table for a given set of measured inputs. A fault detector detects a fault when a difference between actual CQ values and base-case CQ values exceeds a predetermined threshold value for at least one of the CQ values. A fault classifier classifies a detected fault based on which ones of the actual CQ values exceed the interpolated CQ values. The processing unit uses measured inputs selected from the group comprising: chilled water supply temperature; chilled water return temperature; condenser water supply temperature; chilled water flow rate; condenser water flow rate; evaporator saturation temperature; condenser saturation temperature; and compressor discharge temperature. The interpolator may be a General Regression Neural Network, a Probabilistic Neural Network, or a Back Propagation Network.

USE - In HVAC sub systems.

ADVANTAGE - None given.

DESCRIPTION OF DRAWING(S) - The figure shows a block diagram of the diagnosis method.

CHOSEN-DRAWING: Dwg.1/27

TITLE-TERMS: FAULT DETECT DIAGNOSE SUB SYSTEM THERMODYNAMIC CALCULATE CHARACTERISTIC QUANTITY MEASURE INPUT BASE CASE TABLE VALUE FIRST FREE OPERATE PERIOD

DERWENT-CLASS: Q74 Q75 T01 X27

EPI-CODES: T01-G02A2; X27-E01;

SECONDARY-ACC-NO:

Non-CPI Secondary Accession Numbers: 2002-309836